

Edge Detection from Spectral Data

Anne Gelb, Eitan Tadmor

CRPC-TR98644

February 1998

Center for Research on Parallel Computation
Rice University
6100 South Main Street
CRPC - MS 41
Houston, TX 77005

Detection of Edges in Spectral Data*

Anne Gelb[†]Eitan Tadmor[‡]

Abstract

We are interested in the detection of jump discontinuities in piecewise smooth functions which are realized by their spectral data. Specifically, given the Fourier coefficients, $\{\hat{f}_k = a_k + ib_k\}_{k=1}^N$, we form the generalized conjugate partial sum $\tilde{S}_N^\sigma[f](x) = \sum_{k=1}^N \sigma(\frac{k}{N})(a_k \sin kx - b_k \cos kx)$. The classical conjugate partial sum, $\tilde{S}_N[f](x)$, corresponds to $\sigma \equiv 1$ and it is known that $\frac{-\pi}{\log N} \tilde{S}_N[f](x)$ converges to the jump function $[f](x) := f(x+) - f(x-)$; thus, $\frac{-\pi}{\log N} \tilde{S}_N[f](x)$ tends to 'concentrate' near the edges of f . The convergence, however, is at the unacceptably slow rate of order $\mathcal{O}(1/\log N)$.

To accelerate the convergence, thereby creating an effective edge detector, we introduce the so called 'concentration factors', $\sigma_{k,N} = \sigma(\frac{k}{N})$. Our main result shows that an arbitrary $C^2[0, 1]$ non-decreasing $\sigma(x)$ satisfying $\int_0^1 \frac{\sigma(x)}{x} dx \xrightarrow{N \rightarrow \infty} -\pi$, leads to the summability kernel which admits the desired concentration property. To improve over the slowly convergent conjugate Dirichlet kernel (— corresponding to the admissible $\sigma_N(x) \equiv \frac{-\pi}{\log N}$), we demonstrate the examples of two families of concentration functions (depending on free parameters p and α): the so-called Fourier factors, $\sigma_\alpha^F(x) = \frac{-\pi}{Si(\alpha)} \sin \alpha x$, and polynomial factors, $\sigma^p(x) = -p\pi x^p$. These yield effective detectors of (one or more) edges, where both the location and the amplitude of the discontinuities are recovered.

AMS(MOS) subject classification. 42A10, 42A50, 65T10.

Keywords. Fourier expansion, conjugate partial sums, piecewise smoothness, concentration factors.

Contents

| | | |
|----------|--|-----------|
| 1 | Introduction | 2 |
| 2 | The Conjugate Fourier Partial Sum | 5 |
| 3 | Concentration Factors | 10 |
| 3.1 | Introduction | 10 |
| 3.2 | Concentration factors determined by regularization | 11 |
| 3.3 | Concentration factors revisited | 13 |
| 3.4 | Polynomial concentration factors | 16 |
| 4 | Discrete Fourier Expansion | 20 |
| 5 | Concluding remarks | 25 |

*This work was supported by the National Science Foundation under Cooperative Agreement No. 9120008. CRPC-TR 1234567.

[†]CRPC Mail Code 217-50, California Institute of Technology, Pasadena, CA 91125. Email: ag@newvortex.ama.caltech.edu

[‡]Department of Mathematics, UCLA, Los-Angeles CA 90095, and School of Mathematical Sciences, Tel-Aviv University, Tel-Aviv 69978. Email: tadmor@math.ucla.edu

1 Introduction

Smooth functions can be accurately represented by their spectral data. For example, given the Fourier coefficients, $\hat{f}_k = a_k + ib_k$, then the N -term truncated Fourier expansion,

$$S_N[f](x) = \sum_{k=0}^N a_k \cos kx + b_k \sin kx, \quad (1.1)$$

provides a highly accurate representation for smooth f 's. The situation is different, however, in case of piecewise smooth functions, and experience has led to two complementing points of view.

In the first approach, one 'sees' the smooth pieces of f separated by edges of jump discontinuities. The straightforward Fourier expansion in this case experiences the Gibbs' phenomenon: locally, $S_N[f](x)$ 'suffers' $\mathcal{O}(1)$ oscillations in the neighborhoods of the jumps, and globally, there is a slow $\mathcal{O}(\frac{1}{N})$ convergence throughout the smooth pieces. It is still possible to recover a piecewise smooth f from its spectral coefficients, and to retain the superior spectral accuracy; such spectrally accurate recovery is obtained by *filtering* $S_N[f](x)$, and could be carried out either on the Fourier side, e.g., [13],[17], or in physical space, consult [9],[17],[10] and the references therein. As an example for the latter, one introduces a $C_0^1(-1, 1)$ 'bump' function, $B(x)$, such that $B(0) = 1$, and with D_{N^θ} denoting the usual Dirichlet kernel of degree N^θ , $\theta < 1$, we set the mollifier $\psi(x) := B(x)D_{N^\theta}(x)$. Then, replacing $S_N[f]$ with $S_N[f] * \frac{1}{\delta}\psi(\frac{x}{\delta})$ yields a spectrally accurate approximation of $f(x)$ for all x 's which are at least δ -away from the set of jump discontinuities, [9]. Observe that $\psi_\delta(x) = \frac{1}{\delta}\psi(\frac{x}{\delta})$ is a two-sided mollifier supported on $(-\delta, \delta)$ with spectrally small moments. In a series of works, (reviewed in [10]), Gottlieb and Shu used one-sided mollifiers to recover a piecewise smooth f *up to* the discontinuous 'edges'. All these recovery procedures require a priori knowledge of the location of the underlying jump discontinuities. Thus detection of the 'edges' in this approach remains a critical issue.

In a second approach, one is directly interested in 'seeing' the edges of f , edges which are viewed as being 'separated' by pieces of smoothness. Detection of edges in this context are fundamental in a variety of computational algorithms, from spectrally-accurate schemes for capturing shock discontinuities, e.g., [16],[12], to image compression, consult [1],[6] and the references therein. Of course, wavelet expansions are particularly suitable for edge detection: one traces jump discontinuities by 'zooming' through the dyadic scales, consult [15], [5], [14], [6] and the references therein.

In this paper we address the question of edge detection in spectral data. We offer a simple and effective procedure to detect edges, based on *generalized conjugate partial sums* of the form

$$\tilde{S}_N^\sigma[f](x) = \sum_{k=1}^N \sigma\left(\frac{k}{N}\right)(a_k \sin kx - b_k \cos kx).$$

The starting point is the standard conjugate sum, $\tilde{S}_N[f](x)$, corresponding to $\sigma(x) \equiv 1$. The classical result due to Lukács, e.g., [3, §42],[18, §II Theorem 8.13], asserts that $\frac{-\pi}{\log N} \tilde{S}_N[f](x)$ converges to the jump function

$$[f](x) := f(x+) - f(x-),$$

and thus, $\frac{-\pi}{\log N} \tilde{S}_N[f](x)$ tends to 'concentrate' near the edges of f . The convergence, however, is at the unacceptably slow rate of order $\mathcal{O}(1/\log N)$ (indeed, consult Figure (2.1) below). To accelerate the convergence, thereby creating an effective edge detector, we introduce the so called 'concentration factors', $\sigma_{k,N} = \sigma(\frac{k}{N})$. Our main result shows that an arbitrary $C^2[0, 1]$ non-decreasing $\sigma(x)$ satisfying

$$\int_{\frac{1}{N}}^1 \frac{\sigma(x)}{x} dx \xrightarrow{N \rightarrow \infty} -\pi,$$

is 'admissible', in the sense that the corresponding generalized conjugate sum satisfies the concentration property

$$\tilde{S}_N^\sigma[f](x) \xrightarrow{N \rightarrow \infty} [f](x).$$

To demonstrate our above arguments, we consider the following two examples (on $[-\pi, \pi]$):

$$f_a(x) := \cos\left(\frac{x}{2}(2 + \operatorname{sgn} x)\right); \quad f_b(x) := \begin{cases} \cos(x - \frac{x}{2}\operatorname{sgn}(|x| - \frac{\pi}{2})), & x < 0, \\ \cos(\frac{5}{2}x + x\operatorname{sgn}(|x| - \frac{\pi}{2})), & x > 0. \end{cases}$$

In both cases, $f_a(x)$ and $f_b(x)$ are recovered from their Fourier coefficients using the Fourier partial sums $S_N[f](x)$. (both the continuous and the discrete cases are considered) The Gibbs phenomenon is depicted in Figures 1.1 (– the continuous case) and 1.2 (– the discrete case).

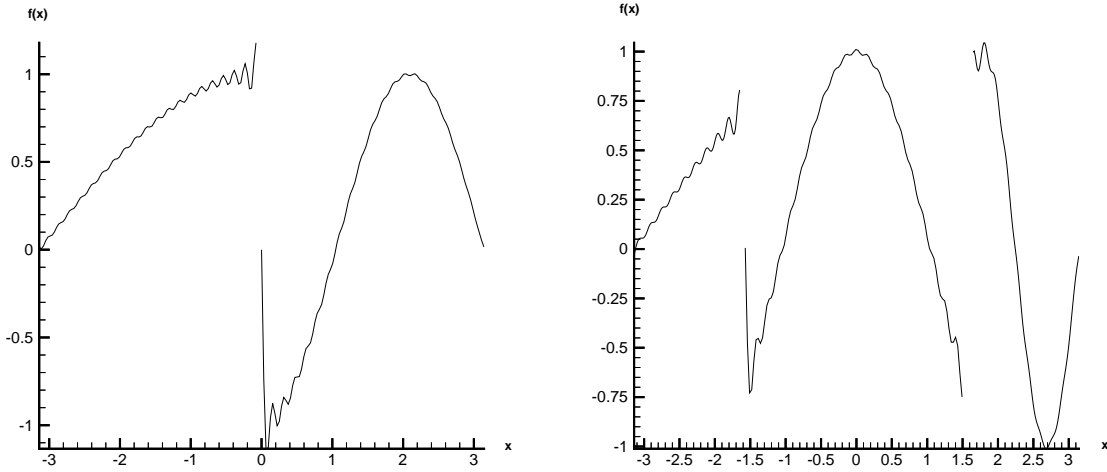


Figure 1.1: Fourier partial sum, $S_{40}[f](x)$, of $f = f_a(x)$ (on left) and $f = f_b(x)$ (on right).

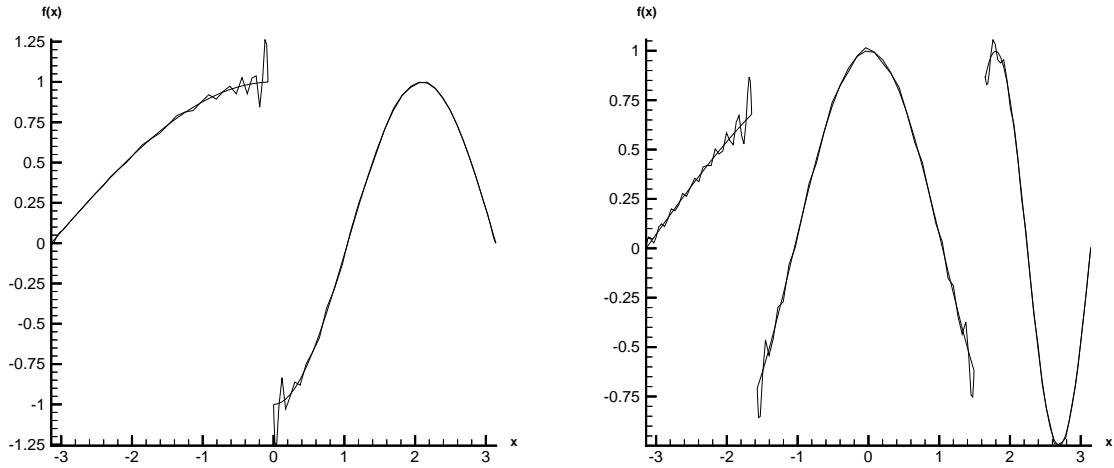


Figure 1.2: Fourier partial sum of $f = f_a(x)$ (on left) and $f = f_b(x)$ (on right) using $N = 40$ discrete Fourier modes, $\hat{f}_k = \frac{\Delta x}{2\pi} \sum_{j=-N}^N f(x_j) e^{ikx_j}$, which are based on the given gridvalues at the $2N + 1$ equidistant gridpoints x_j .

Figure 1.3 shows the reconstruction of a piecewise smooth function using the one-sided mollifier presented in [11]. Here $f_a(x)$ and $f_b(x)$ are recovered from their continuous Fourier coefficients (Figure 1.3) and from their discrete Fourier coefficients (Figure 1.4). The recovery requires the location of the jump discontinuities.

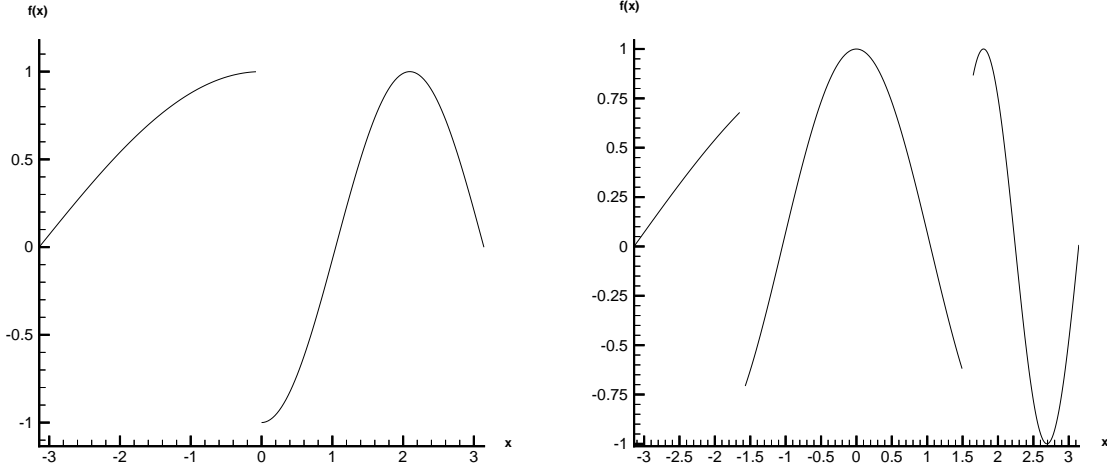


Figure 1.3: Reconstruction of a piecewise continuous functions, $f = f_a(x)$ (on left) and $f = f_b(x)$ (on right), after filtering $S_{40}[f](x)$ with one-sided mollifier.

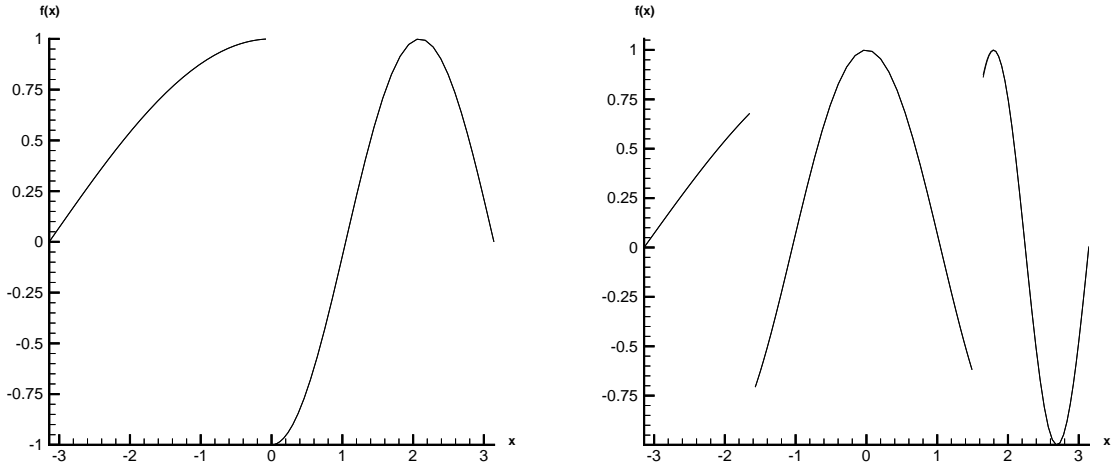


Figure 1.4: Reconstruction of a piecewise continuous functions, $f = f_a(x)$ (on left) and $f = f_b(x)$ (on right), after filtering their discrete Fourier interpolant (of degree $N = 40$) with one-sided mollifier.

Finally, Figure 1.5 shows the detection of these jump discontinuities using our proposed generalized conjugate sum. In this case, we use the concentration function $\sigma(x) = -\pi x$. Both the location and the amplitude of the jump discontinuities, $[f_a](0) = -2$ and $[f_b](\pm\pi/2) = \pm\sqrt{2}$ are clearly identified.

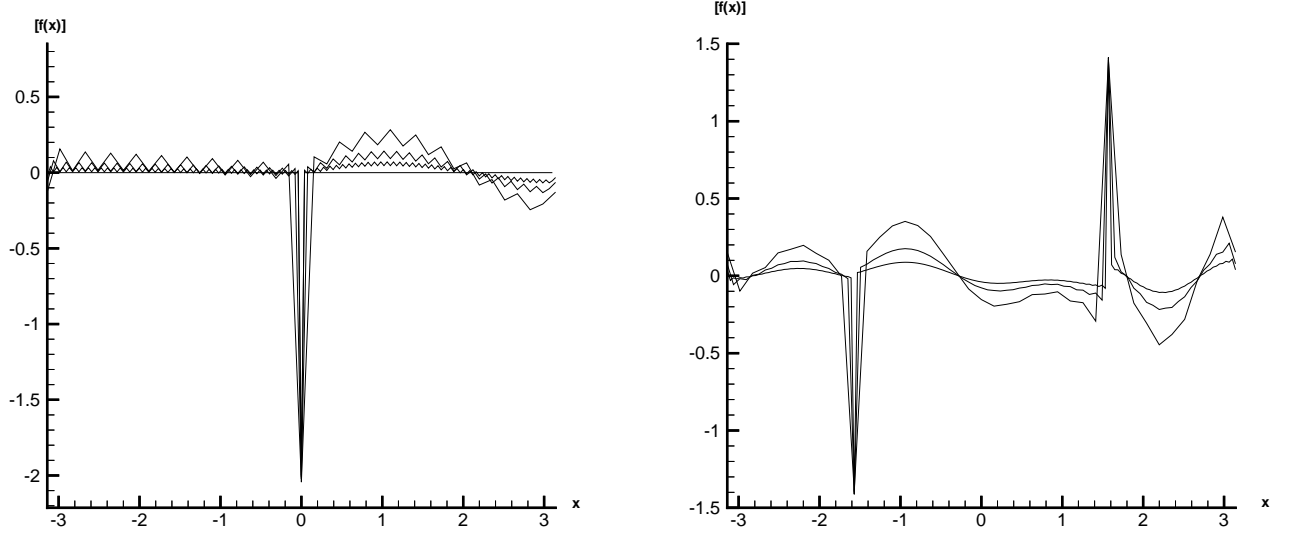


Figure 1.5: Detection of discontinuous edges using the conjugate sum, $\tilde{S}_N^\sigma[f](x) = -\sum \sigma(\frac{k}{N}) i \operatorname{sgn}(k) \hat{f}_k e^{ikx}$ using $N = 20, 40$ and 80 modes, and based on the first degree polynomial concentration function, $\sigma^{p_1}(x) = -\pi x$.

The paper is organized as follows. The so called *concentration property* of the basic conjugate partial sum, $\tilde{S}_N[f]$ is reviewed in §2. In §3 we devise our new, more general approach for locating jump discontinuities based on the concentration property of the *generalized* conjugate partial sums, $\tilde{S}_N^\sigma[f]$. Here we provide a systematic study of concentration factors, $\sigma(\frac{k}{N})$, and their improved resolution of the limiting jump function $[f](x)$. Finally, in §4 we extend our theory for the analogous discrete case.

Acknowledgments. The research of E. Tadmor was supported in part by NSF Grant DMS97-06827 and ONR Grant N00014-91-J-1076.

2 The Conjugate Fourier Partial Sum

Let $f(x)$ be a 2π -periodic piecewise smooth function, with a single jump discontinuity at $x = \xi$, whose associated jump value is defined as

$$[f](\xi) := f(\xi+) - f(\xi-). \quad (2.1)$$

Given the Fourier coefficients of $f(x)$

$$\begin{Bmatrix} a_k \\ b_k \end{Bmatrix} = \frac{1}{\pi} \int_{-\pi}^{\pi} f(t) \begin{Bmatrix} \cos kt \\ \sin kt \end{Bmatrix} dt, \quad (2.2)$$

our goal is to *identify* the jump discontinuities, i.e., to locate the jump discontinuities and to accurately evaluate their associated jump values. The key to locating the discontinuities lies in the relationship between the conjugate Fourier partial sum and the jump discontinuities.

The conjugate Fourier partial sum is given by

$$\tilde{S}_N[f](x) := \sum_{k=1}^N a_k \sin kx - b_k \cos kx. \quad (2.3)$$

Equivalently, $\tilde{S}_N[f](x)$ can be written as

$$\tilde{S}_N[f](x) = f * \frac{1}{\pi} \tilde{D}_N = \frac{1}{\pi} \int_{-\pi}^{\pi} f(t) \tilde{D}_N(x-t) dt, \quad (2.4)$$

where \tilde{D}_N is the conjugate Dirichlet Kernel

$$\tilde{D}_N(t) = \sum_{k=1}^N \sin kt = \frac{\cos \frac{t}{2} - \cos(N + \frac{1}{2})t}{2 \sin \frac{t}{2}}. \quad (2.5)$$

We recall that the support of the conjugate Fourier partial sum $\tilde{S}_N[f](x)$ approaches the singular support of $f(x)$ as $N \rightarrow \infty$, e.g., [3, §42], [18, §II Theorem 8.13]. This will be referred to as the *concentration property* of $\tilde{S}_N[f](x)$. To illustrate the concentration property of $\tilde{S}_N[f](x)$, we offer the specific example of the saw-tooth function

$$\Phi_\xi(x) = \begin{cases} -\frac{\pi+x}{2}, & -\pi \leq x < \xi \\ -\frac{x-\pi}{2}, & \xi \leq x \leq \pi. \end{cases}$$

In this case $[f](\xi) = \pi$ and the conjugate Fourier partial sum is

$$\tilde{S}_N[\Phi_\xi](x) = -\sum_{k=1}^N \frac{\cos k(x-\xi)}{k}.$$

The concentration property of $\tilde{S}_N[\Phi_\xi](x)$ can be deduced from the following:

Assertion 2.1 *We have*

$$\frac{1}{\log N} \sum_{k=1}^N \frac{\cos k(x-\xi)}{k} \rightarrow \delta_\xi(x) := \begin{cases} 1 & \text{if } x = \xi \\ 0 & \text{otherwise.} \end{cases} \quad (2.6)$$

The proof is immediate. Let $D_N(y)$ denote the usual Dirichlet kernel

$$D_N(y) = \sum_{k=0}^N \cos ky. \quad (2.7)$$

Summation by parts yields

$$\begin{aligned} \sum_{k=1}^N \frac{\cos k(x-\xi)}{k} &= \sum_{k=1}^N \frac{1}{k} (D_k(x-\xi) - D_{k-1}(x-\xi)) \\ &= \sum_{k=1}^N \frac{D_k(x-\xi)}{k(k+1)} + \frac{D_N(x-\xi)}{N} - D_0(x-\xi). \end{aligned}$$

Since $|D_N(y)| \leq \frac{1}{2 \sin |\frac{y}{2}|}$, we have $\sum_{k=1}^N \frac{\cos k(x-\xi)}{k} \leq (\frac{\pi^2}{6} + \frac{1}{N}) \frac{1}{2 \sin |\frac{x-\xi}{2}|} + \frac{1}{2}$, and (2.6) follows for $x \neq \xi$.

Of course, for $x = \xi$ we have $\frac{1}{\log N} \sum_{k=1}^N \frac{\cos k(x-\xi)}{k} \rightarrow 1$, as asserted. \blacksquare

This special case of the saw-tooth function can be generalized to any piecewise smooth function, as told by

Theorem 2.1 *(On the concentration property.) Let $f(x)$ be a 2π -periodic piecewise smooth function with a single discontinuity at $x = \xi$. Then*

$$-\frac{\pi}{\log N} \tilde{S}_N[f](x) \rightarrow [f](x) \delta_\xi(x) = \begin{cases} [f](x) & x = \xi \\ 0 & \text{otherwise.} \end{cases} \quad (2.8)$$

We shall offer two proofs for this theorem. The first approach is a straightforward extension of the concentration property of the saw-tooth function asserted in (2.6), along the lines of [18, §II Theorem 8.13].

Proof. Consider the function $g(x) \equiv f(x) - \frac{[f](\xi)}{\pi} \Phi_\xi(x)$, where $\Phi_\xi(x)$ is the saw-tooth function with a π -jump at $x = \xi$. Consequently, $g(x)$ is a C^0 function which vanishes at $x = \xi$. By (2.4), the conjugate sum of $g(x)$ equals

$$\tilde{S}_N[g](x) = \frac{1}{\pi} \int_{-\pi}^{\pi} g(t) \tilde{D}_N(x-t) dt. \quad (2.9)$$

Applying the standard upper-bounds of $\tilde{D}_N(t)$ in (2.5), $|\tilde{D}_N(t)| \leq \min(N, \frac{2}{|t|})$, and the fact that $g(x)$ is a continuous function with $g(\xi) = 0$, we obtain

$$\begin{aligned} |\tilde{S}_N[g](\xi)| &\leq \frac{2}{\pi} \int_{\xi}^{\xi+\pi} |g(t)| |\tilde{D}_N(\xi-t)| dt \\ &\leq \frac{2}{\pi} \int_{\xi}^{\xi+\frac{\pi}{N}} |g(t)| |\tilde{D}_N(\xi-t)| dt + \frac{2}{\pi} \int_{\xi+\frac{\pi}{N}}^{\xi+\pi} |g(t)| |\tilde{D}_N(\xi-t)| dt \\ &\leq \frac{2N}{\pi} \int_{\xi}^{\xi+\frac{\pi}{N}} |g(t)| dt + \frac{4}{\pi} \int_{\xi+\frac{\pi}{N}}^{\xi+\pi} \frac{|g(t)|}{|\xi-t|} dt \\ &= o(1) + o(\log N) = o(\log N). \end{aligned}$$

By the definition of $g(x)$, Assertion 2.1, and the previous estimate it follows that

$$\begin{aligned} -\frac{\pi}{\log N} \tilde{S}_N[f](x) &\equiv -\frac{\pi}{\log N} \tilde{S}_N[g](x) - \frac{[f](\xi)}{\log N} \tilde{S}_N[\Phi_\xi](x) \\ &= -\frac{\pi}{\log N} o(\log N) + [f](\xi) \delta_\xi(x) + o(1), \end{aligned}$$

and we are done. ■

Theorem 2.1 says that

$$f * \frac{-\pi}{\log N} \tilde{D}_N(x) \xrightarrow{N \rightarrow \infty} [f](x) \delta_\xi(x).$$

We would like to point out that the scaled conjugate Dirichlet kernel, $\frac{-\pi}{\log N} \tilde{D}_N$, is just one example for a broader class of admissible “conjugate” kernels which induce the concentration property. This brings us to the following:

Definition 2.1 (*Admissible kernels*) *We say that a “conjugate” kernel, \tilde{K}_N , is admissible if it satisfies the following four properties:*

$$\mathcal{P}1 : \quad \tilde{K}_N \text{ is odd}; \quad (2.10)$$

$$\mathcal{P}2 : \quad \lim_{N \rightarrow \infty} \int_0^\pi \tilde{K}_N(x) dx \rightarrow -1; \quad (2.11)$$

$$\mathcal{P}3 : \quad \tilde{K}_N(x) = C \cdot \frac{\cos(N + \frac{1}{2})t}{2\pi \sin(\frac{t}{2})} + \tilde{R}_N(x), \quad \|\tilde{R}_N\|_{L^1} \leq \text{Const} \quad (2.12)$$

$$\mathcal{P}4 : \quad \lim_{N \rightarrow \infty} \sup_{|x| > \delta > 0} |\tilde{R}_N(x)| \rightarrow 0, \quad \forall \text{ fixed } \delta > 0. \quad (2.13)$$

Clearly, the scaled conjugate Dirichlet kernel, $\frac{-\pi}{\log N} \tilde{D}_N(x)$, is admissible: indeed, in this case properties (P3) and (P4) hold with $\tilde{K}_N = \tilde{R}_N = \frac{-\pi}{\log N} \tilde{D}_N$ and $C = 0$. Properties (P3) and (P4) are motivated by the fact that unlike the scaled Dirichlet kernel, the generalized conjugate kernels we shall meet later on are *not* uniformly integrable.

Our second proof of concentration property applies to general admissible kernels. Of course, the result applies to piecewise smooth functions with more than just a single discontinuity. We now need to specify our precise notion of *piecewise smoothness*, making

Assumption 2.1 [*Piecewise smoothness.*] $f(x)$ is piecewise smooth in the sense of having finite number of jump discontinuities where $[f](x) \neq 0$, and such that $\forall x$'s

$$\frac{f(x+t) - f(x-t) - [f](x)}{t} \in L^1[0, \pi]. \quad (2.14)$$

Thus, piecewise smooth f 's with smooth pieces which are Hölder of any order $\alpha > 0$ will suffice. (To be precise, we may allow appropriate Besov regularity, yet in actual computation we cannot *resolve* but a finite number of discontinuities...)

Theorem 2.2 (*The concentration property revisited.*) Let $f(x)$ be a piecewise-smooth function, (2.14), and let $J = \{\xi\}$ denote the set of its jump discontinuities. Consider the generalized conjugate partial sum

$$\tilde{S}_N^K[f] := f * \tilde{K}_N = \int_{-\pi}^{\pi} f(t) \tilde{K}_N(x-t) dt,$$

where \tilde{K}_N is an admissible kernel satisfying properties (P1) – (P4) in (2.10) – (2.13). Then

$$\tilde{S}_N^K[f](x) \rightarrow [f](x) \delta_J(x) = \begin{cases} [f](\xi) & x = \xi \in J \\ 0 & \text{otherwise.} \end{cases} \quad (2.15)$$

Remark. Note that the convergence asserted in (2.15) need not be uniform.

Proof. Since by property (P1) in (2.10) \tilde{K}_N is odd, we can rewrite the corresponding conjugate partial sum \tilde{S}_N as

$$\tilde{S}_N^K[f](x) = - \int_0^{\pi} [f(x+t) - f(x-t)] \tilde{K}_N(t) dt. \quad (2.16)$$

Define the 'local variation' $j(t) := [f](x) - (f(x+t) - f(x-t))$, and split (2.16) into four contributions,

$$\begin{aligned} \tilde{S}_N^K[f](x) &= - \int_0^{\pi} [f(x+t) - f(x-t)] \tilde{K}_N(t) dt \\ &= -[f](x) \cdot \int_0^{\pi} \tilde{K}_N(t) dt + C \int_0^{\pi} \frac{j(t)}{2\pi \sin(\frac{t}{2})} \cos(N + \frac{1}{2})t dt \\ &\quad + \int_0^{\delta} j(t) \tilde{R}_N(t) dt + \int_{\delta}^{\pi} j(t) \tilde{R}_N(t) dt \\ &=: I_N + II_N + III_N + IV_N. \end{aligned}$$

Property (P2) in (2.11) yields that the first term approaches the jump $[f](x)$,

$$I_N = -[f](x) \cdot \int_0^{\pi} \tilde{K}_N(t) dt \rightarrow [f](x), \quad N \rightarrow \infty;$$

By piecewise smoothness, $\frac{j(t)}{\sin t/2} \in L^1[0, \pi]$ and by Riemann-Lebesgue $II_N \xrightarrow{N \rightarrow \infty} 0$. Given an ε , we can find

$\delta = \delta(\varepsilon)$ such that $\sup_{(0, \delta)} |j(t)| \leq \varepsilon$, and since $\|\tilde{R}_N\|_{L^1}$ is bounded by (P3) in (2.12), it follows that the third term III_N can be made as small as we please independently of N ,

$$|III_N| = \left| \int_0^{\delta} j(t) \tilde{R}_N(t) dt \right| \leq \|\tilde{R}_N\|_{L^1} \cdot \sup_{(0, \delta)} |j(t)| \leq \text{Const} \cdot \varepsilon;$$

And finally, property (P4) in (2.13) implies that $\sup_{t>\delta>0} |\tilde{R}_N(t)|$ can be made arbitrarily small for N large enough, $N > N_0(\delta(\varepsilon))$, and hence

$$IV_N = \int_{\delta}^{\pi} j(t) \tilde{R}_N(t) dt \leq Const \cdot \sup_{t>\delta>0} |\tilde{R}_N(t)| \xrightarrow{N \rightarrow \infty} 0.$$

Thus the convolution of f with any admissible kernel \tilde{K}_N satisfies the concentration property. ■

The following example illustrates Theorem 2.2 for the conjugate Fourier partial sum, $\tilde{S}_N^D[f](x) = \frac{-\pi}{\log N} \tilde{S}_N[f](x)$. In this case, $\tilde{K}_N = \frac{-1}{\log N} \tilde{D}_N$ corresponds to the “canonical” conjugate kernel given in Theorem 2.1. Clearly, it is an odd kernel with unit mass over $(0, \pi)$, so (P1) and (P2) hold. The estimate $|\tilde{D}_N(t)| \leq \min(N, \frac{2}{|t|})$ implies that $\tilde{K}_N = \frac{-1}{\log N} \tilde{D}_N$, also satisfies properties (P3) and (P4); indeed with $\tilde{R}_N(x) = \frac{-1}{\log N} \tilde{D}_N(x)$ we find

- $\int_{-\pi}^{\pi} |\tilde{R}_N(t)| dt \leq 2 \left[\int_0^{\frac{1}{N}} + \int_{\frac{1}{N}}^{\pi} \right] |\tilde{R}_N(t)| dt \leq Const$, yielding (P3) in (2.12); and
- $|\tilde{R}_N(t)| \leq \frac{1}{\log N} |\tilde{D}_N(t)| \leq \frac{2}{|t| \log N}$, satisfying (P4) in (2.13).

We close this section with

Example 2.1

$$f(x) = \begin{cases} \sin \frac{x+\pi}{2}, & -\pi \leq x < 0 \\ \sin \frac{3x+\pi}{2}, & 0 < x \leq \pi. \end{cases}$$

Here $\xi = 0$ and $[f](\xi) = -2$.

It is clear from Figure 2.1 that $\tilde{S}_N^D[f](x) = \frac{-\pi}{\log N} \tilde{S}_N[f](x)$ does in fact locate the singularity point and approximate the jump value there. Furthermore, in agreement with Theorems 2.1 and 2.2, the numerical convergence rate is $\mathcal{O}(\frac{1}{\log N})$ – both at the discontinuity point and away from it. In particular, the slow convergence is exhibited in Figure 2.1 where $N = 80$ modes do *not* recover the correct amplitude of the jump, $[f](0) = -2$. The improvement of this slow logarithmic convergence rate will occupy our discussion in the remaining sections. Note that naive straightforward smoothing does not improve the convergence rate. In fact, the resolution of the smoothed conjugate Dirichlet kernel at the discontinuity is less sharp, as shown in Figure 2.1 where an exponential smoothing filter is used by pre-multiplying $\hat{f}_k \rightarrow \exp(\frac{\alpha|\frac{k}{N}|^{\beta}}{|k|-N}) \hat{f}_k$. The results are similar for other smoothing filters.

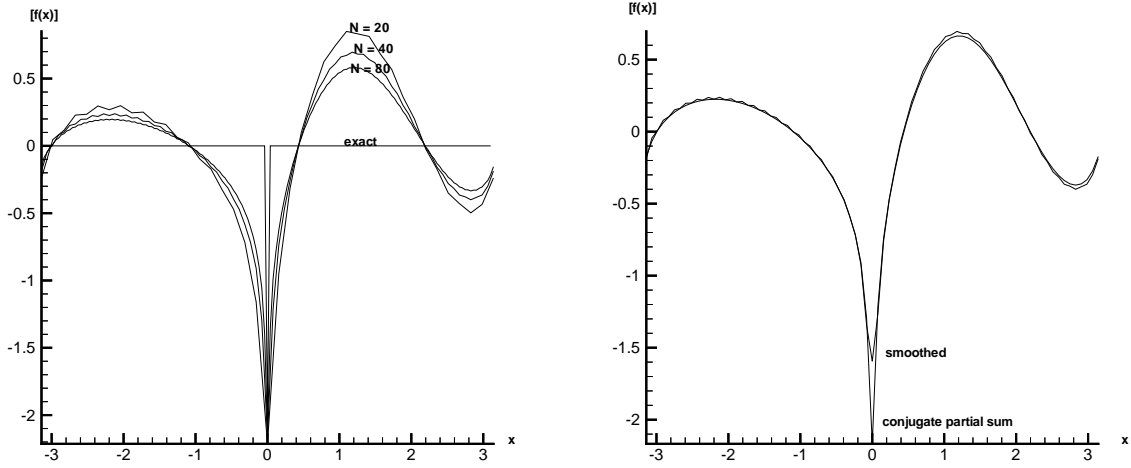


Figure 2.1: The conjugate Fourier partial sum $\tilde{S}_N^D[f](x) = \frac{-\pi}{\log N} \tilde{S}_N[f](x)$ computed with $N = 40$ modes. Here, $f = f_a(x)$ given in Example 2.1, experiences a single jump, $[f](0) = -2$. Before smoothing (on the left) and after smoothing (on the right).

3 Concentration Factors

3.1 Introduction

Consider a piecewise smooth function $f(x)$ with a single discontinuity at $x = \xi$. We introduce a *generalized* conjugate partial sum of the form¹

$$\tilde{S}_N^\sigma[f](x) = \sum_{k=1}^N \sigma_{k,N} (a_k \sin kx - b_k \cos kx). \quad (3.1)$$

Here $\sigma = \{\sigma_{k,N}\}$ are free summability parameters to be determined so that the *concentration property* similar to (2.8) holds:

$$\tilde{S}_N^\sigma[f](x) \rightarrow [f](x) \delta_\xi(x). \quad (3.2)$$

For example, $\sigma_{k,N} \equiv \frac{-\pi}{\log N}$ corresponds to the canonical conjugate Fourier partial sums $\tilde{S}_N^\sigma[f](x) = \frac{-\pi}{\log N} \tilde{S}_N[f](x)$. In this case, (3.2) holds in view of Theorem 2.1. It is clear that these σ 's influence the convergence *rate* associated with the concentration property of $\tilde{S}_N^\sigma[f](x)$. We refer to σ as the *concentration factors* of $\tilde{S}_N^\sigma[f](x)$.

As a preliminary step, we begin by estimating the Fourier coefficients to their leading order. Integration by parts yields

$$a_k \sim -\frac{1}{\pi k} [f](\xi) \sin k\xi + O\left(\frac{1}{k^2}\right), \quad b_k \sim \frac{1}{\pi k} [f](\xi) \cos k\xi + O\left(\frac{1}{k^2}\right). \quad (3.3)$$

Substituting (3.3) into (3.1) yields

$$\tilde{S}_N^\sigma[f](x) = -[f](\xi) \sum_{k=1}^N \frac{\sigma_{k,N} \cos k(x - \xi)}{\pi k} + \mathcal{O}\left(\frac{1}{N}\right). \quad (3.4)$$

Therefore, the desired concentration property of $\tilde{S}_N^\sigma[f](x)$ in (3.2) amounts to:

¹We use the notation \tilde{S}_N^K and \tilde{S}_N^σ to indicate the dependence on both the concentration kernel \tilde{K}_N and the concentration factor $\sigma_{k,N}$. This 'abuse' of notation will be clarified in §3.3 below.

Assertion 3.1 *Let $\sigma = \{\sigma_{k,N}\}$ be the concentration factors with the corresponding generalized conjugate partial sum $\tilde{S}_N^g[f](x) = \sum_{k=1}^N \sigma_{k,N}(a_k \sin kx - b_k \cos kx)$. Then the concentration property (3.2) requires*

$$-\sum_{k=1}^N \frac{\sigma_{k,N} \cos k(x-\xi)}{\pi k} \rightarrow \delta_\xi(x). \quad (3.5)$$

Before turning to our general discussion on concentration factors, we note the following.

Remarks.

1. The scaled conjugate Fourier partial sum $\frac{-\pi}{\log N} \tilde{S}_N[f](x) = f * \frac{-1}{\log N} \tilde{D}_N$ corresponds to the concentration factors $\sigma_{k,N} \equiv \frac{-\pi}{\log N}$. We thus denote

$$\sigma_{k,N}^D \equiv \frac{-\pi}{\log N}, \quad (3.6)$$

as the *Dirichlet concentration factors*, and note that they are independent of k . In this case, Assertion 2.1 states that (3.5) holds with an error term of order $O(\frac{1}{\log N})$, yielding the concentration statement of Theorem 2.1 and in agreement with Assertion 3.1.

2. As a consequence of the leading order expansion in (3.3), the highest accuracy that can be obtained in (3.5) for locating the jump discontinuity $x = \xi$ is first order, $\mathcal{O}(\frac{1}{N})$. Faster convergence of (3.5) may be achieved by further expanding the Fourier coefficients in terms of higher derivatives. This is considered for the particular methods examined in [2] and [7], and is also suitable for our general method. Here, we are concerned with improving the first order convergence rate, and we note that higher orders can be handled in a similar manner.
3. The concentration factors to be determined, σ , must show an *overall* improved accuracy for (3.2). More specifically, we seek concentration factors which, beyond improving the convergence rate, will lead to $\tilde{S}_N^g[f](x)$ having better resolution of the singular support of $f(x)$. This will be clarified by the differences between the various concentration factors outlined below.
4. Although only functions with a single point of discontinuity are considered here, our results are easily extended to include any piecewise smooth functions (along the lines of Theorem 2.2), as will be seen in Example 3.1 below.

3.2 Concentration factors determined by regularization

One possible approach to improving the convergence rate of (3.2) is to (weakly) regularize the partial sums in (3.5) by defining the regularized indicator function, $\delta_\xi^\epsilon(x)$,

$$\delta_\xi^\epsilon(x) := \begin{cases} 1, & |x - \xi| \leq \epsilon \\ 0, & \epsilon < |x - \xi| \leq \pi. \end{cases} \quad (3.7)$$

Observe that $\delta_\xi^\epsilon(x)$ has an even Fourier expansion in $(x - \xi)$, whose Fourier partial sum is given by

$$S_N[\delta_\xi^\epsilon(x)](x) = \frac{2\epsilon}{\pi} + \sum_{k=1}^N 2 \sin k\epsilon \frac{\cos k(x - \xi)}{\pi k}. \quad (3.8)$$

Compared with Assertion 3.1, we can identify the summation on the right of (3.8) with concentration factors of the form $\sigma_{k,N} = c \sin k\epsilon_N$; here we consider vanishing $\epsilon_N = \frac{\alpha}{N}$ which depends on a fixed free parameter α . The scaling coefficient, c , should be determined so that the concentration characterization in (3.5) holds, $-\sum_{k=1}^N \frac{\sigma_{k,N}}{\pi k} \rightarrow 1$. It follows that $c = -\pi/Si(\alpha)$ with $Si(\alpha)$ denoting the usual $Si(\alpha) = \int_0^\alpha \frac{\sin x}{x} dx$.

In summary, we arrive at the family of concentration factors (depending on α)

$$\sigma_{k,N}^F \equiv \frac{-\pi}{Si(\alpha)} \sin k\epsilon_N, \quad \epsilon_N = \frac{\alpha}{N}. \quad (3.9a)$$

We refer to these as the *Fourier concentration factors*, denoted $\{\sigma_{k,N}^F\}$, since they are in fact, (proportional to) the Fourier coefficients of $\delta_\xi^\epsilon(x)$. For this choice of Fourier concentration factors (3.5) holds with a convergence rate of order $\mathcal{O}(\epsilon_N)$.

The results for Example 2.1 using the Fourier concentration factors, $\sigma_{k,N}^F$, are shown in Figure 3.1. Compared with the ‘concentration-free’ conjugate Dirichlet kernel in Figure 2.1, the improved resolution of the discontinuity at $x = 0$ is evident.

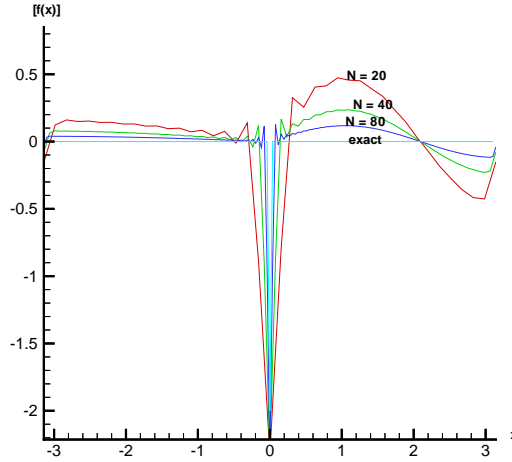


Figure 3.1: Jump value obtained by applying the Fourier concentration factors, (3.9_α), $\alpha = 1$, to Example 2.1. The exact jump is $[f](0) = -2$.

In this context, we recall an alternative approach to locating jump discontinuities as suggested in Banerjee and Geer [2]. As described below, the method in [2] is based on estimating the Gibbs’ overshoots which occur exactly at the points of discontinuity. We shall see that the method in [2] in fact leads to a particular set of ‘Fourier’ concentration factors.

We briefly describe the method given in [2]. Starting with Fourier partial sum $S_N[f](x) = \sum_{k=0}^N a_k \cos kx + b_k \sin kx$, it yields the familiar Gibbs’ overshoot at $x = \xi$, of size

$$\lim_{N \rightarrow \infty} [S_N[f](\xi+) - S_N[f](\xi-)] = \frac{2Si(\pi)}{\pi} [f(\xi)],$$

where $\frac{2Si(\pi)}{\pi} = \frac{2}{\pi} \int_0^\pi \frac{\sin u}{u} du \approx 1.17898$ accounts for 18% Gibbs’ overshoot. It follows that

$$\frac{S_N[f](x + \frac{\pi}{N}) - S_N[f](x - \frac{\pi}{N})}{\frac{2}{\pi} Si(\pi)} \rightarrow \begin{cases} [f](\xi) & \text{for } x = \xi \\ 0 & \text{otherwise.} \end{cases} \quad (3.10)$$

Thus, the (scaled) *difference* of the Gibbs’ picks at $x \pm \frac{\pi}{N}$ ‘concentrate’ at the discontinuity. In [2], the location of ξ and an approximation of $[f](\xi)$ were recovered by direct evaluation of (3.10).

How can this procedure based on (3.10) be interpreted within our general framework? Inserting the leading order terms of the Fourier coefficients in (3.3), it follows that

$$\frac{S_N[f](x + \frac{\pi}{N}) - S_N[f](x - \frac{\pi}{N})}{\frac{2}{\pi} Si(\pi)} \sim [f](\xi) \frac{-\pi}{Si(\pi)} \sum_{k=1}^N \sin \frac{\pi k}{N} \frac{\cos k(x - \xi)}{\pi k}. \quad (3.11)$$

Compared with the characterization of the concentration property in (3.5), one recognizes the summation on the right of (3.11) as a generalized conjugate Fourier partial sum associated with the concentration factors

$\sigma_{k,N} \equiv \frac{-\pi}{Si(\pi)} \sin k \frac{\pi}{N}$. In fact, these fall into the special category of Fourier concentration factors in (3.9 _{α}), corresponding to $\alpha = \pi$. Thus the approach in [2] given in (3.10), concurs with the so-called ‘‘Gibbs’’ concentration factors, $\sigma_{k,N}^G$, given by

$$\sigma_{k,N}^G \equiv \frac{-\pi}{Si(\pi)} \sin \frac{\pi k}{N}. \quad (3.12)$$

The results are depicted in Figure 3.2.

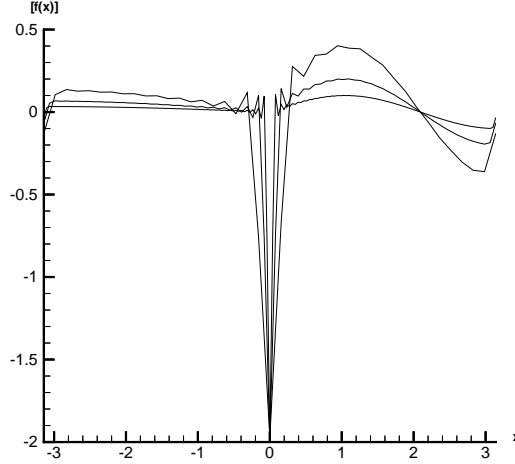


Figure 3.2: Jump value obtained by applying the Gibbs concentration factors to Example 2.1 with $N = 20, 40$ and 80 modes. The exact jump is $[f](0) = -2$.

3.3 Concentration factors revisited

Bearing in mind the concentration factors σ determined thus far, we revisit (3.1) to determine general criteria that will guarantee the concentration property (3.2). We start by considering the concentration factors $\sigma_{k,N} = \sigma(\frac{k}{N})$, where $\sigma(x) = \sigma_N(x)$ is a *concentration function* which is yet to be determined. Note that we still allow $\sigma(x) = \sigma_N(x)$ to depend on N . In the generic case, however, $\sigma(x)$ is independent of N , (e.g., $\sigma_\alpha^F(x) \sim \sin(\alpha x)$ for the Fourier concentration factors in (3.9 _{α})), and so we omit the sub-index N .

We start by summing

$$\tilde{S}_N^\sigma[f](x) := \sum_{k=1}^N \sigma\left(\frac{k}{N}\right) (a_k \sin kx - b_k \cos kx) = - \int_{-\pi}^{\pi} f(t) \frac{1}{\pi} \sum_{k=1}^N \sigma\left(\frac{k}{N}\right) \sin k(x-t) dt, \quad (3.13)$$

which leads to generalized conjugate kernels of the form

$$\tilde{K}_N^\sigma(t) = \frac{-1}{\pi} \sum_{k=1}^N \sigma\left(\frac{k}{N}\right) \sin kt. \quad (3.14)$$

We ask ourselves when such kernels are admissible in the sense of satisfying the four properties outlined in Definition 2.1, so that by Theorem 2.2 the concentration property holds:

$$\tilde{S}_N^\sigma[f](x) \equiv f * \tilde{K}_N^\sigma \rightarrow [f](x) \delta_\xi(x). \quad (3.15)$$

In the language of Assertion 3.1, one focuses here at $f(x) \equiv 1$, where (3.15) boils down to (3.5)

$$\tilde{S}_N[1](x) = 1 * \tilde{K}_N^\sigma = - \sum_{k=1}^N \frac{\sigma(\frac{k}{N})}{\pi k} \cos k(x - \xi) \longrightarrow \delta_\xi(x). \quad (3.16)$$

Clearly, the $\tilde{K}_N^\sigma(t)$ are odd so property (P1) holds; moreover, with the minimal requirement of bounded concentration factors, $|\sum_1^N \sigma(\frac{k}{N}) \sin kt| \leq \text{Const} \cdot N$ and hence $\|\tilde{K}_N^\sigma\|_{L^1(0,\pi)}$ is bounded if $\|\tilde{K}_N^\sigma\|_{L^1(1/N,\pi)}$ is. Namely we start with

Corollary 3.1 *Consider the conjugate kernel*

$$\tilde{K}_N^\sigma(t) = \frac{-1}{\pi} \sum_{k=1}^N \sigma(\frac{k}{N}) \sin kt,$$

associated with bounded concentration factors, $\sigma(\frac{k}{N})$. Then \tilde{K}_N^σ is an admissible kernel (and hence the concentration property (3.15) holds), if the following conditions are fulfilled:

$$\mathcal{P}2' : \quad \lim_{N \rightarrow \infty} \left[\sum_{k=1}^N \frac{\sigma(\frac{k}{N})}{k} (1 - (-1)^k) \right] = -\pi; \quad (3.17)$$

$$\mathcal{P}3' : \quad \tilde{R}_N^\sigma(t) = C \frac{\cos(N + \frac{1}{2})t}{2\pi \sin(\frac{t}{2})} + \tilde{R}_N(x), \quad \int_{\frac{1}{N}}^\pi |\tilde{R}_N^\sigma(t)| dt \leq \text{Const}; \quad (3.18)$$

$$\mathcal{P}4' : \quad \lim_{N \rightarrow \infty} \sup_{t > \delta > 0} |\tilde{R}_N^\sigma(t)| = 0, \quad \forall \text{ fixed } \delta > 0. \quad (3.19)$$

Next, we provide easily checkable characterizations of properties (P2')–(P4'). We summarize our results (adding minimal requirements on the smoothness of the concentration function $\sigma(x)$) in the following two assertions. The first deals with the *total mass* of the concentration kernel, \tilde{K}_N^σ .

Assertion 3.2 *Assume that the concentration function $\sigma(x) \equiv \sigma_N(x) \in C^1[0,1]$ satisfies*

$$\int_{\frac{1}{N}}^1 \frac{\sigma_N(x)}{x} dx \rightarrow -\pi, \quad \sum_{j=1}^N \frac{|\sigma(\frac{j}{N})|}{j^2} \xrightarrow{N \rightarrow \infty} 0. \quad (3.20)$$

Then property (P2') and hence (P2) hold, i.e., $\lim_{N \rightarrow \infty} \int_0^\pi \tilde{K}_N^\sigma(t) dt = -1$.

Remark. If $\frac{\sigma(x)}{x}$ is integrable then the summation encountered in property (P2') is in fact the Riemann sum of

$$\sum_{k=1}^N \frac{\sigma(\frac{k}{N})}{k} (1 - (-1)^k) = \sum_{j=0}^{N/2} \frac{\sigma(\frac{2j+1}{N})}{\frac{2j+1}{N}} \frac{2}{N} \sim \int_0^1 \frac{\sigma(x)}{x} dx.$$

And thus we find that if $\sigma(x) \in L^1([0,1], \frac{dx}{x})$ satisfies

$$\int_0^1 \frac{\sigma_N(x)}{x} dx \rightarrow -\pi, \quad (3.21)$$

then property (P2') in (3.17) holds. The (slight) refinement asserted in (3.20) extends to L^1 -weak kernels which are excluded by (3.21).

Proof. Set $x_j := \frac{j}{N}$. By continuity, $\int_{x_{2j-1}}^{x_{2j+1}} \frac{\sigma(x)}{x} dx = [\sigma(x_{2j-1}) + \mathcal{O}(\frac{1}{N})] \cdot \int_{x_{2j-1}}^{x_{2j+1}} \frac{1}{x} dx$. Summing such terms we find

$$\begin{aligned} \int_{\frac{1}{N}}^1 \frac{\sigma_N(x)}{x} dx &= \sum_{j=1}^{N/2} \int_{x_{2j-1}}^{x_{2j+1}} \frac{\sigma(x)}{x} dx = \\ &= \sum_{j=1}^{N/2} [\sigma(x_{2j-1}) + \mathcal{O}(\frac{1}{N})] \times [\frac{2}{2j-1} + \mathcal{O}(\frac{1}{j^2})] = \\ &= \sum_{k=1}^N \frac{\sigma(\frac{k}{N})}{k} [1 - (-1)^k] + \sum_1^{N/2} \frac{\sigma(x_j)}{j^2} + \mathcal{O}(\frac{1}{N}), \end{aligned}$$

and the result follows. \blacksquare

Our next assertion, dealing with properties (P3')–(P4'), provides a sharp upper-bound on the *amplitude* of the conjugate kernel, $\tilde{K}_N^\sigma(x) - \sigma(1) \frac{\cos(N + \frac{1}{2})t}{2\pi \sin(\frac{t}{2})}$.

Assertion 3.3 *Consider the conjugate kernel $\tilde{K}_N^\sigma(t) = \frac{-1}{\pi} \sum_{k=1}^N \sigma(\frac{k}{N}) \sin kt$, with concentration function $\sigma(x) \in C^2[0, 1]$. Then the following estimate holds*

$$|\tilde{K}_N(t) - \sigma(1) \frac{\cos(N + \frac{1}{2})t}{2\pi \sin(\frac{t}{2})}| \leq \left[\|\sigma\|_{C^2} + \text{Const.} \right] \frac{1}{N|t|^2} + \left[\left| \sigma\left(\frac{1}{N}\right) \right| + \frac{1}{N} |\sigma(1)| \right] \frac{1}{|t|}. \quad (3.22)$$

Remark. Thus, (3.22) shows that if $|\sigma(\frac{1}{N})| \leq \text{Const.} \frac{1}{\log N}$ then both properties (P3') and (P4') hold.

Proof. Twice summation by parts leads to the identity (recall the notation $x_k := \frac{k}{N}$)

$$\begin{aligned} 4 \sin^2\left(\frac{t}{2}\right) \sum_{k=1}^N \sigma(x_k) \sin kt &\equiv - \sum_{k=1}^{N-1} \left[\sigma(x_{k+1}) - \sigma(x_k) \right] \cdot [\sin(k+1)t - \sin kt] + \\ &\quad + 2\sigma(1) \sin \frac{t}{2} \cos(N + \frac{1}{2})t - 2\sigma(x_1) \sin \frac{t}{2} \cos \frac{t}{2} = \\ &\equiv \sum_{k=1}^{N-2} \left[\sigma(x_{k+2}) - 2\sigma(x_{k+1}) + \sigma(x_k) \right] \sin(k+1)t + \\ &\quad + \left[\sigma(1) - \sigma(x_{N-1}) \right] \sin Nt - \left[\sigma(x_2) - \sigma(x_1) \right] \sin t \\ &\quad + 2\sigma(1) \sin \frac{t}{2} \cos(N + \frac{1}{2})t - 2\sigma(x_1) \sin \frac{t}{2} \cos \frac{t}{2}. \end{aligned} \quad (3.23)$$

By the C^2 smoothness of $\sigma(x)$ we find

$$|\tilde{K}_N^\sigma(t)| \leq \|\sigma\|_{C^2} \frac{1}{Nt^2} + \left[\left| \sigma\left(\frac{1}{N}\right) \right| + |\sigma(1)| \right] \frac{1}{|t|}. \quad (3.24)$$

To conclude the proof we consider the special example of $\sigma(x) = x$: the corresponding conjugate kernel (with $\sigma_{k,N} = \frac{k}{N}$) reads $\tilde{K}_N^x(t) = \frac{-1}{\pi} \sum_{k=1}^N \frac{k}{N} \sin kt$ and it coincides with the differentiated Dirichlet kernel in (2.7), $\frac{1}{\pi N} D'_N(t)$,

$$\tilde{K}_N^x(t) = \frac{-1}{\pi} \sum_{k=1}^N \frac{k}{N} \sin kt = \frac{N + \frac{1}{2}}{2\pi N} \frac{\cos(N + \frac{1}{2})t}{2\pi \sin(\frac{t}{2})} - \frac{1}{4\pi N} \frac{\cos \frac{t}{2} \sin(N + \frac{1}{2})t}{\sin^2(\frac{t}{2})}. \quad (3.25)$$

Now we decompose

$$\tilde{K}_N^\sigma(t) \equiv \left[\tilde{K}_N^\sigma(t) - \sigma(1) \tilde{K}_N^x(t) \right] + \sigma(1) \tilde{K}_N^x(t).$$

The first difference on the right is a conjugate kernel associated with concentration function $\mu(x) := \sigma(x) - \sigma(1)x$. Application of (3.24) to $\tilde{K}_N^\mu(t)$ implies the upperbound asserted in (3.22). Also, by (3.25), $\tilde{K}_N^x(t) - \frac{N + \frac{1}{2}}{2\pi N} \frac{\cos(N + \frac{1}{2})t}{2\pi \sin(\frac{t}{2})}$ does not exceed $\frac{1}{Nt^2}$, and the result follows. \blacksquare

We summarize our last two assertions, by stating our main

Theorem 3.1 (*Admissible kernels*) *Consider the conjugate kernel $\tilde{K}_N^\sigma(t) = \frac{-1}{\pi} \sum_{k=1}^N \sigma(\frac{k}{N}) \sin kt$ associated with a $C^2[0, 1]$ concentration function $\sigma(x)$, such that $|\sigma(\frac{1}{N})| \leq \text{Const.} \frac{1}{\log N}$. Assume*

$$\int_{\frac{1}{N}}^1 \frac{\sigma_N(x)}{x} dx \rightarrow -\pi, \quad (3.26)$$

$$\sum_{j=1}^N \frac{|\sigma(\frac{j}{N})|}{j^2} \xrightarrow{N \rightarrow \infty} 0. \quad (3.27)$$

Then $\tilde{K}_N^\sigma(t)$ is an admissible kernel, so that $\tilde{S}_N^\sigma[f](x) = f * \tilde{K}_N^\sigma$ satisfies the concentration property, $\tilde{S}_N^\sigma[f](x) \xrightarrow{N \rightarrow \infty} [f](x)\delta_\xi(x)$.

Remark. If $\sigma(x)$ is non-decreasing, then necessarily, $|\sigma(\frac{1}{N})| \leq \text{Const.} \frac{1}{\log N}$ for (3.17) to hold, and in this case (3.27) is fulfilled. If also $\frac{\sigma(x)}{\pi x} \in L^1[0, 1]$, then admissibility requires only the scaling condition

$$\int_0^1 \frac{\sigma(x)}{x} dx = -\pi. \quad (3.28)$$

It is easy to see from the above discussion that $\sigma_{k,N}^D, \sigma_{k,N}^F$ (and in particular, $\sigma_{k,N}^G$) are admissible concentration factors: in the first case, the Fourier concentration factors $\sigma_N(x) \equiv \frac{-\pi}{\log N}$ satisfy (3.27) (and note that in this case $\frac{\sigma(x)}{x}$ is only *weak*- L^1 so that we need the refinement of (3.20)); in the second case of Fourier concentration factors, $\sigma_\alpha^F(x) = \frac{-\pi}{Si(\alpha)} \sin \alpha x$ satisfies (3.28).

3.4 Polynomial concentration factors

Guided by the results of Theorem 3.1 we define a family of what we refer to as “polynomial” concentration factors, based on concentration functions, $\sigma^p(x) = -p\pi x^p$. The first two members in this family yield

- First degree polynomial concentration factors ($\sigma(x) = -\pi x$)

$$\sigma_{k,N}^{p_1} \equiv -\frac{\pi k}{N} \quad (3.29)$$

- Second degree polynomial concentration factors ($\sigma(x) = -2\pi x^2$)

$$\sigma_{k,N}^{p_2} \equiv -\frac{2\pi k^2}{N(N+1)}. \quad (3.30)$$

Clearly $\sigma^p(x) = -p\pi x^p$ are admissible by Theorem 3.1 and hence the concentration property holds. We note in passing that the generalized conjugate sums associated with the polynomial concentration factors, σ^p , coincide with the differentiated Fourier partial sums,

$$\tilde{S}_N^{\sigma^{2p+1}}[f](x) = -\frac{\pi(2p+1)}{N^{2p+1}} \sum_{k=1}^N k^{2p+1} (a_k \sin kx - b_k \cos kx) = (-1)^p \frac{\pi(2p+1)}{N^{2p+1}} \frac{d^{2p+1}}{dx^{2p+1}} S_N[f](x).$$

The corresponding concentration property then reads

$$(-1)^p \frac{\pi(2p+1)}{N^{2p+1}} S_N^{(2p+1)}[f](x) \rightarrow [f](x). \quad (3.31_p)$$

The special case $p = 0$ was already referred to in the proof of Assertion 3.3, where we made use of the identity $\tilde{K}_N^x(t) \equiv \frac{1}{\pi N} D'_N(t)$, and the corresponding concentration property, (3.31_p) with $p = 0$ goes back to Fejér, [18, §III Theorem 9.3].

To gain better insight into their *overall* improved accuracy, we analyze the behavior of $\tilde{S}_N^{\sigma^p}[1](x) = 1 * \tilde{K}_N^{\sigma^p}(x)$ for x 's away from the assumed jump discontinuity at $x = \xi$, consult (3.5). To this end, we let $\rho := x - \xi$ and rewrite the sum (3.5) corresponding to $\sigma_{k,N}^{p_1}$ as

$$\tilde{S}_N^{\sigma^{p_1}}[1](x) = \frac{1}{N} \sum_{k=1}^N \cos k\rho = \frac{\sin \frac{N\rho}{2} \cos \frac{(N+1)\rho}{2}}{N \sin \frac{\rho}{2}}, \quad \rho = x - \xi.$$

Substituting in the discrete values $\rho_l = \frac{\pi(l-N)}{N}$ for $l = 1, \dots, 2N-1$, yields

$$\tilde{S}_N^{\sigma^{p_1}}[1](x_l) = \frac{\sin \frac{\pi(l-N)}{2} \cos \frac{(N+1)\pi(l-N)}{2N}}{N \sin \frac{\pi(l-N)}{2N}} = \begin{cases} 0 & l \text{ is even} \\ \frac{(-1)^l}{N} & l \text{ is odd.} \end{cases}$$

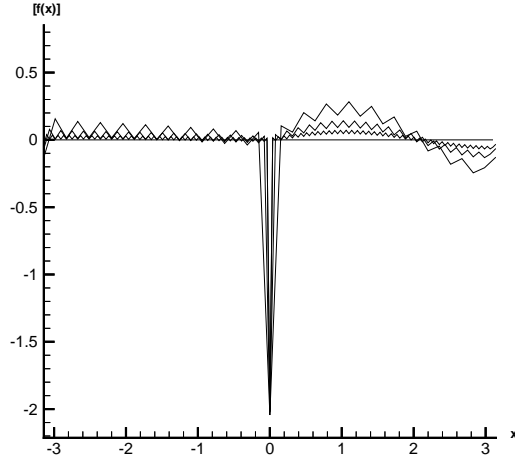


Figure 3.3: Jump value obtained by applying the first order polynomial concentration factors, $\sigma^{p_1}(\frac{k}{N})$, to Example 2.1 with $N = 20, 40$ and 80 modes. The exact jump is $[f](0) = -2$.

The uniform convergence is clearly depicted in Figure 3.3 by the oscillatory behavior between the odd and even gridpoints. It is important to clarify that the convergence at x away from the point of discontinuity does not depend on the value of $x - \xi$, but rather on its distance from an x_l with an odd or even index. It follows that the convergence rate for (3.2) corresponding to the first order polynomial factors, $\sigma^{p_1}(\frac{k}{N})$, is the same for all odd (even) x_l , regardless of proximity to the points of discontinuity.

For the second order polynomial factors, $\sigma^{p_2}(\frac{k}{N})$, we rewrite (3.5) as

$$\begin{aligned} \tilde{S}_N^{\sigma^{p_2}}[1](x) &= \sum_{k=1}^N \frac{2k \cos k\rho}{N(N+1)} = -\frac{2}{N(N+1)} \sum_{k=1}^N \frac{\sin \frac{k\rho}{2} \cos \frac{(k+1)\rho}{2}}{\sin \frac{\rho}{2}} + \frac{1}{N} \sum_{k=1}^N \cos k\rho \\ &= -\frac{\cot \frac{k\rho}{2}}{N(N+1)} \sum_{k=1}^N \sin k\rho + \frac{2}{N(N+1)} \sum_{k=1}^N \sin^2 \frac{k\rho}{2} + \frac{1}{N} \sum_{k=1}^N \cos k\rho, \quad \rho = x - \xi. \end{aligned}$$

Using the closed formulas

$$\sum_{k=1}^N \cos k\rho = \frac{\sin \frac{k\rho}{2} \cos \frac{(k+1)\rho}{2}}{\sin \frac{\rho}{2}}, \quad \sum_{k=1}^N \sin k\rho = \frac{\cos \frac{\rho}{2}}{2 \sin \frac{\rho}{2}} - \frac{\cos (N + \frac{1}{2})\rho}{2 \sin \frac{\rho}{2}},$$

we substitute the discrete values $\rho_l = \frac{\pi(l-N)}{N}$ and apply a fair amount of algebra to obtain

$$\tilde{S}_N^{\sigma^{p_2}}[1](x_l) = \begin{cases} O(\frac{1}{N^2}) & \text{if } l \text{ even} \\ O(\frac{1}{N}) + O(\frac{\cot^2 \frac{\rho_l}{2}}{N^2}) & \text{if } l \text{ odd.} \end{cases}$$

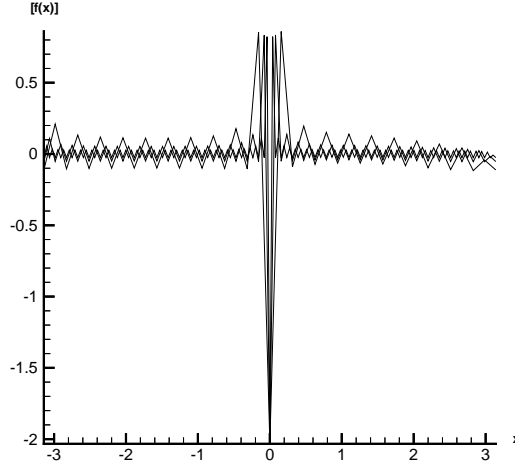


Figure 3.4: Jump value obtained by applying the second order polynomial concentration factors to Example 2.1 with $N = 20, 40$ and 80 modes. The exact jump is $[f](0) = -2$.

Thus the second degree polynomial factors attain second order convergence (but only at the even discretization points). It is also oscillatory, and due to the added error term $\mathcal{O}(\frac{\cot^2 \frac{\theta_l}{2}}{N^2})$ at the odd points, it is dependent on the proximity of the jump discontinuity ξ to the discretized value of x_l . This error implies that the convergence is worse near the points of discontinuity and the lack of uniform convergence is depicted in Figure 3.4. On a positive note, $\tilde{S}_N^{\sigma^{p_2}}[f](x) \rightarrow 0$ more rapidly outside the immediate proximity of the discontinuity point, which may be helpful in identifying jump discontinuities for functions with stronger variation, as will be seen in Example 3.1. We note that there are higher order polynomial factors corresponding to admissible kernels \tilde{K}_N^σ that may work as well.

Table 3.1 compares different concentration factors for Example 2.1, with the first row showing the magnitude of error for $[f](0)$ and the second row comparing the average error for $[f](x \neq 0)$.

| $[f](x)$ | $\sigma_{k,N}^D$ | $\sigma_{k,N}^F$ | $\sigma_{k,N}^G$ | $\sigma_{k,N}^{p_1}$ | $\sigma_{k,N}^{p_2}$ |
|---------------|------------------|------------------|------------------|----------------------|----------------------|
| at $x = 0$ | 0.168 | 2.0E-02 | 6.5E-03 | 2.4E-02 | 1.1E-02 |
| at $x \neq 0$ | 0.326 | 5.9E-02 | 0.11 | 5.5E-02 | 6.7E-02 |

Table 3.1: Error comparison for Example 2.1 with $N = 40$ modes. First row: Absolute error for $[f](0) = -2$. Second row: average error for $[f](x \neq 0) = 0$.

As expected, the worst case is with the Dirichlet concentration factors. The results are comparable for $\sigma_{k,N}^F$ and $\sigma_{k,N}^G$. Overall, the polynomial concentration factors work better than the Fourier concentration factors, and it is not surprising that $\sigma_{k,N}^{p_2}$ produces a slower convergence rate averaged over x 's $\neq 0$, due to the contribution of order $\mathcal{O}(\frac{\cot^2 \frac{\theta_l}{2}}{N^2})$ which prevents uniform convergence near the point of discontinuity.

Until now we have only discussed functions with one discontinuity. Example 3.1 demonstrates the detection of edges for a function with two discontinuities.

Example 3.1 *We consider*

$$f(x) = \begin{cases} \cos \frac{x}{2}, & -\pi \leq x < -\frac{\pi}{2} \\ \cos \frac{3x}{2}, & -\frac{\pi}{2} \leq x < \frac{\pi}{2} \\ \cos \frac{7x}{2}, & \frac{\pi}{2} \leq x \leq \pi. \end{cases}$$

Here $\xi_1 = -\frac{\pi}{2}$, $\xi_2 = \frac{\pi}{2}$, and $[f](\xi_2) = -[f](\xi_1) = \sqrt{2}$.

Figure 3.5 displays the results for Example 3.1 using different concentration factors. The polynomial concentration factors work better than the Fourier concentration factors, and the fast convergence of $\tilde{S}_N^\sigma[f](x)$ for $\{\sigma_{k,N}^{p_2}\}$ is more evident than in the first example.

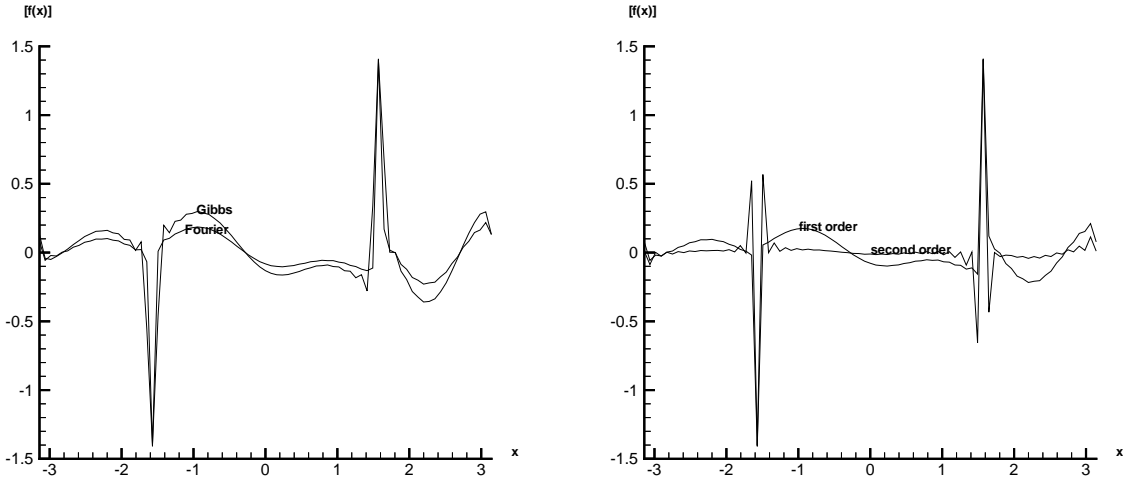


Figure 3.5: Jump value obtained by different values of $\sigma_\alpha^F(\frac{k}{N})$ with $\alpha = 1$ and $\alpha = \pi$ (on the left) and $\sigma^p(\frac{k}{N})$ with $p = 1$ and $p = 2$ (on the right), when applied to Example 3.1 with $N = 40$ modes. The exact solution is $[f](\pm\frac{\pi}{2}) = \pm\sqrt{2}$, and $[f](x \neq \pm\frac{\pi}{2}) = 0$.

Table 3.2 compares the different concentration factors for $[f](\xi_1)$, while Table 3.3 compares the average error of $[f](x \neq \xi_1, \xi_2)$. The tables indicate that the polynomial concentration factors yield better results than their Fourier counterparts. Here we see that $\sigma_{k,N}^{p_2}$ yields better average accuracy away from the points of discontinuity than $\sigma_{k,N}^{p_1}$. In this case, the smooth 'pieces' in Example 3.1, exhibit stronger variation than before and the faster convergence of $\tilde{S}_N^\sigma[f](x)$ corresponding to $\sigma_{k,N}^{p_2}$ away from the discontinuities plays a more dominant role.

| N | $\sigma_{k,N}^D$ | $\sigma_{k,N}^F$ | $\sigma_{k,N}^G$ | $\sigma_{k,N}^{p_1}$ | $\sigma_{k,N}^{p_2}$ |
|-----|------------------|------------------|------------------|----------------------|----------------------|
| 20 | 0.453 | 9.2E-03 | 7.0E-02 | 5.4E-02 | .150 |
| 40 | 0.372 | 1.0E-02 | 1.6E-02 | 3.1E-02 | 6.0E-02 |
| 80 | 0.315 | 6.5E-03 | 4.0E-03 | 1.7E-03 | 2.5E-02 |

Table 3.2: Absolute error for Example 3.1 at $x = -\frac{\pi}{2}$.

| N | $\sigma_{k,N}^D$ | $\sigma_{k,N}^F$ | $\sigma_{k,N}^G$ | $\sigma_{k,N}^{p_1}$ | $\sigma_{k,N}^{p_2}$ |
|-----|------------------|------------------|------------------|----------------------|----------------------|
| 20 | 0.466 | .195 | .319 | .188 | .119 |
| 40 | 0.382 | 9.6E-02 | .171 | 9.2E-02 | 4.8E-02 |
| 80 | 0.327 | 4.8E-02 | 8.9E-02 | 4.5E-02 | 2.1E-02 |

Table 3.3: Average error for Example 3.1 away from the discontinuities.

We mention again that while the estimates above are at best first order, they can be improved to $O(\frac{1}{N^2})$ by substituting the results of $[f](\xi)$ back into (3.3) and applying another integration by parts. Finally we emphasize that the possibilities for σ are not exhausted, and that other concentration factors may provide better results.

4 Discrete Fourier Expansion

Suppose we are given the discrete gridvalues $f(x_j)$ defined at the $2N + 1$ equidistant points, $x_j := -\pi + (j + N)\Delta x$, with $\Delta x := \frac{2\pi}{2N+1}$. The discrete Fourier expansion approximation is given by

$$T_N[f](x) = \sum_{k=0}^N \alpha_k \cos kx + \beta_k \sin kx,$$

where the corresponding $2N + 1$ discrete Fourier coefficients based on those $2N + 1$ equidistant gridvalues are defined as

$$\begin{aligned} \alpha_k &= \frac{\Delta x}{\pi} \sum_{j=-N}^N f(x_j) \cos kx_j, \quad 0 \leq k \leq N \\ \beta_k &= \frac{\Delta x}{\pi} \sum_{j=-N}^N f(x_j) \sin kx_j, \quad 1 \leq k \leq N. \end{aligned} \tag{4.1}$$

The discrete conjugate Fourier partial sum is therefore

$$\tilde{T}_N[f](x) = \sum_{k=1}^N \alpha_k \sin kx - \beta_k \cos kx. \tag{4.2}$$

In the discrete case, every gridvalue experiences a jump discontinuity. The jumps that are of order $\mathcal{O}(\Delta x)$ are acceptable, but the $\mathcal{O}(1)$ jumps indicate a jump discontinuity in the underlying function $f(x)$. Hence, in the discrete case we identify a jump discontinuity at ξ by its enclosed gridcell, $[x_j, x_{j+1}]$, which is characterized by the asymptotic statement (

$$f(x_{j+1}) - f(x_j) = \begin{cases} [f](\xi) + \mathcal{O}(\Delta x) & \text{for } j = j_\xi : \xi \in [x_j, x_{j+1}] \\ \mathcal{O}(\Delta x) & \text{for other } j\text{'s } \neq j_\xi. \end{cases} \tag{4.3}$$

Of course, this asymptotic statement, (4.3), may serve as an edge detector based the given *gridvalues*, $\{f(x_j)\}_{j=-N}^N$. We now seek alternative edge detectors based the the discrete Fourier coefficients, $\{\alpha_k, \beta_k\}_{k=1}^N$, analogue to our study of the continuous case in §3.

As a starting point, we point out the inadequacy of the concentration factors studied in §3, $\sigma(\frac{k}{N})$, in the present context of *discrete* Fourier expansion (4.2). Figure 4.1 shows the results for the discrete data of Example 3.1. The discrepancy in Figures 3.5 and 4.1 clearly indicates that the concentration factors determined in §3 are not applicable here. A separate (but closely related) study is required for discrete concentration factors.

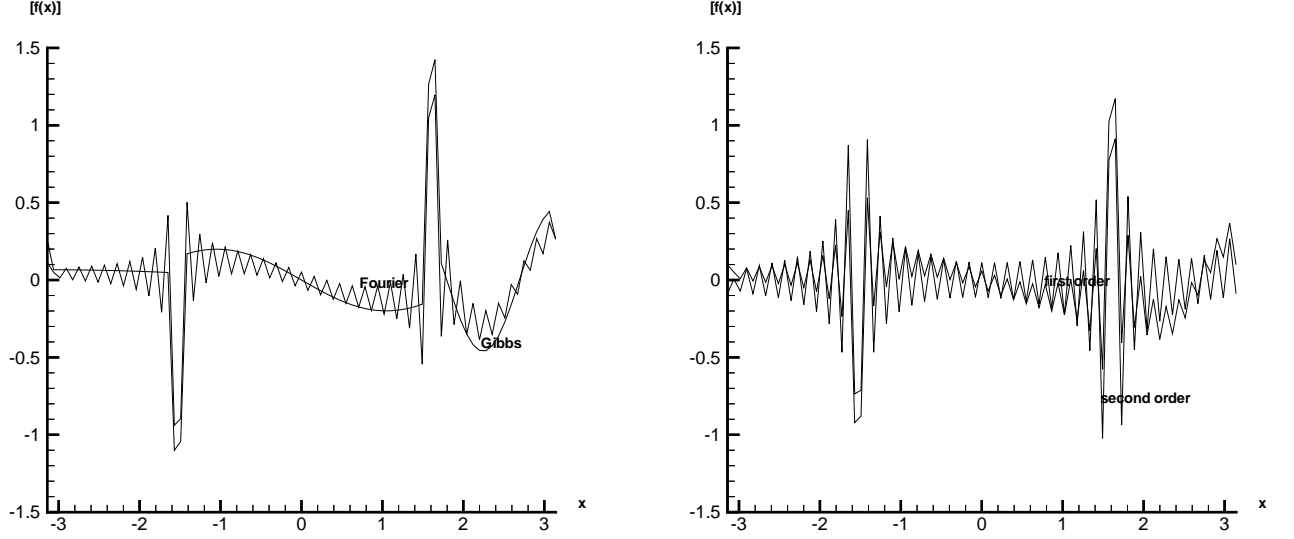


Figure 4.1: Jump values obtained by applying different “continuous” concentration factors to the discrete Fourier coefficients for Example 3.1 with $N = 40$ modes. The exact solution experiences two jumps $[f](\pm \frac{\pi}{2}) = \pm \sqrt{2}$.

To analyze the discrete case, we follow our framework in §3. We introduce concentration factors $\tau_{k,N}$ and consider the (discrete) generalized conjugate sums

$$\tilde{T}_N^\tau[f](x) := \sum_{k=1}^N \tau_{k,N} (\alpha_k \sin kx - \beta_k \cos kx). \quad (4.4)$$

Summing by parts the discrete Fourier coefficients we find

$$\begin{aligned} \alpha_k &= \frac{\Delta x}{2\pi \sin k \frac{\Delta x}{2}} \sum_{j=-N}^N \sin kx_{j+\frac{1}{2}} [f(x_j) - f(x_{j+1})], \\ \beta_k &= \frac{\Delta x}{2\pi \sin k \frac{\Delta x}{2}} \sum_{j=-N}^N \cos kx_{j+\frac{1}{2}} [f(x_{j+1}) - f(x_j)]. \end{aligned}$$

Let $\xi_{j+\frac{1}{2}} = x_{j_\xi+\frac{1}{2}}$ denote the midpoint of the cell $[x_{j_\xi}, x_{j_\xi+1}]$ which encloses the discontinuity at $x = \xi$. Applying (4.3) to the discrete Fourier coefficients in (4.1) gives

$$\begin{aligned} \alpha_k &= -\frac{\Delta x}{2\pi \sin k \frac{\Delta x}{2}} [f(\xi_{j+\frac{1}{2}})] \sin k\xi + \mathcal{O}(\Delta x), \\ \beta_k &= \frac{\Delta x}{2\pi \sin k \frac{\Delta x}{2}} [f(\xi_{j+\frac{1}{2}})] \cos k\xi + \mathcal{O}(\Delta x), \end{aligned} \quad (4.5)$$

and substituting (4.5) into (4.4) leads to

$$\tilde{T}_N[f](x) = -[f](\xi) \sum_{k=1}^N \frac{\Delta x \cdot \tau_{k,N}}{2\pi \sin k \frac{\Delta x}{2}} \cos k(x - \xi_{j+\frac{1}{2}}) + \mathcal{O}(\Delta x). \quad (4.6)$$

Observe that as $\Delta x \rightarrow 0$, the discrete conjugate sum $\tilde{T}_N[f](x)$ approaches the corresponding continuous conjugate sum $\tilde{S}_N^\tau[f](x)$. In fact, by comparing (4.6) with $\tilde{S}_N^\tau[f](x)$ in (3.4),

$$\tilde{S}_N^\tau[f](x) = -[f](\xi) \sum_{k=1}^N \frac{\sigma_{k,N}}{\pi k} \cos k(x - \xi) + \mathcal{O}\left(\frac{1}{N}\right),$$

we see that the concentration property of the discrete conjugate Fourier partial sum is a direct analogue of the continuous case. Of course, in the discrete case, we do not identify the exact location of the underlying discontinuity at $x = \xi$, but rather the location of the discrete cell which encloses this discontinuity which is realized here in terms of its midpoint at $x = \xi_{j+\frac{1}{2}}$.

We arrive at the following discrete analogue of our Theorem 3.1 for detecting edges in spectral of piecewise smooth functions. In this discrete context, piecewise smoothness refers to piecewise C^2 functions, i.e., we refer to f 's with finite number of jump discontinuities where $[f](x) \neq 0$, such that (2.14) is strengthened into

$$f(x+t) - f(x-t) - [f](x) \in C^2[0, \pi]. \quad (4.7)$$

Theorem 4.1 *Let $f(x)$ be a piecewise smooth function, (4.7), and let $J = \{\xi\}$ denote the set of its jump discontinuities. Given the discrete Fourier coefficients, $\{\alpha_k + i\beta_k\}_{k=1}^N$, we consider the generalized discrete conjugate partial sum*

$$\tilde{T}_N^\tau[f](x) = \sum_{k=1}^N \tau_{k,N} (\alpha_k \sin kx - \beta_k \cos kx) \quad (4.8)$$

corresponding to the discrete concentration factors $\tau = \{\tau_{k,N}\} = \tau(\frac{k}{N})$. If $\tau_{k,N}$ are related to admissible continuous concentration factors $\sigma_{k,N}$ in (3.1)

$$\tau_{k,N} = \frac{\sin(k\frac{\Delta x}{2})}{k\frac{\Delta x}{2}} \sigma_{k,N}, \quad \Delta x = \frac{2\pi}{2N+1}, \quad (4.9)$$

then $\tilde{T}_N^\tau[f](x)$ satisfies the concentration property

$$\tilde{T}_N^\tau[f](x) \rightarrow [f](\xi) \delta_J(x). \quad (4.10)$$

Furthermore, the direct analogue to the continuous case offers a more general result:

Theorem 4.2 *Consider a $C^2[0, 1]$ discrete concentration function $\tau(x)$ such that $|\tau(\frac{1}{N})| \leq \text{Const.} \frac{1}{\log N}$. Then $\tau_{k,N} = \tau(\frac{k}{N})$ are admissible and the concentration property is fulfilled,*

$$\tilde{T}_N^\tau[f](x) \rightarrow [f](\xi) \delta_J(x),$$

if the following conditions are met:

$$\int_{\frac{1}{N}}^1 \frac{\tau_N(x)}{2 \sin \pi \frac{x}{2}} dx \xrightarrow{N \rightarrow \infty} -1; \quad (4.11)$$

$$\sum_{j=1}^N \frac{|\tau(\frac{j}{N})|}{j^2} \xrightarrow{N \rightarrow \infty} 0. \quad (4.12)$$

All of the continuous concentration factors $\sigma = \{\sigma_{k,N}\}$ from §3 can therefore be 'converted' into discrete concentration factors $\tau = \{\tau_{k,N}\}$ up to a scaling factor of $\sin(k\frac{\Delta x}{2})/(k\frac{\Delta x}{2})$:

1. Dirichlet concentration factors

$$\tau_k^D \equiv \frac{-2}{k\Delta x \log N} \sin k \frac{\Delta x}{2} \quad (4.13)$$

2. Fourier concentration factors

$$\tau_k^F = \frac{-2}{k\Delta x \text{Si}(\alpha)} \sin k \frac{\Delta x}{2} \sin(k \frac{\alpha}{N}); \quad (4.14_\alpha)$$

3. Gibbs concentration factors

$$\tau_k^G \equiv \frac{-2}{k\Delta x Si(\pi)} \sin k \frac{\Delta x}{2} \sin \frac{\pi k}{N}; \quad (4.15)$$

4. First order polynomial concentration factors

$$\tau_k^{p_1} \equiv \frac{-2\pi}{\Delta x N} \sin k \frac{\Delta x}{2}; \quad (4.16)$$

5. Second order polynomial concentration factors

$$\tau_k^{p_2} \equiv \frac{-4k\pi}{\Delta x N(N+1)} \sin k \frac{\Delta x}{2}; \quad (4.17)$$

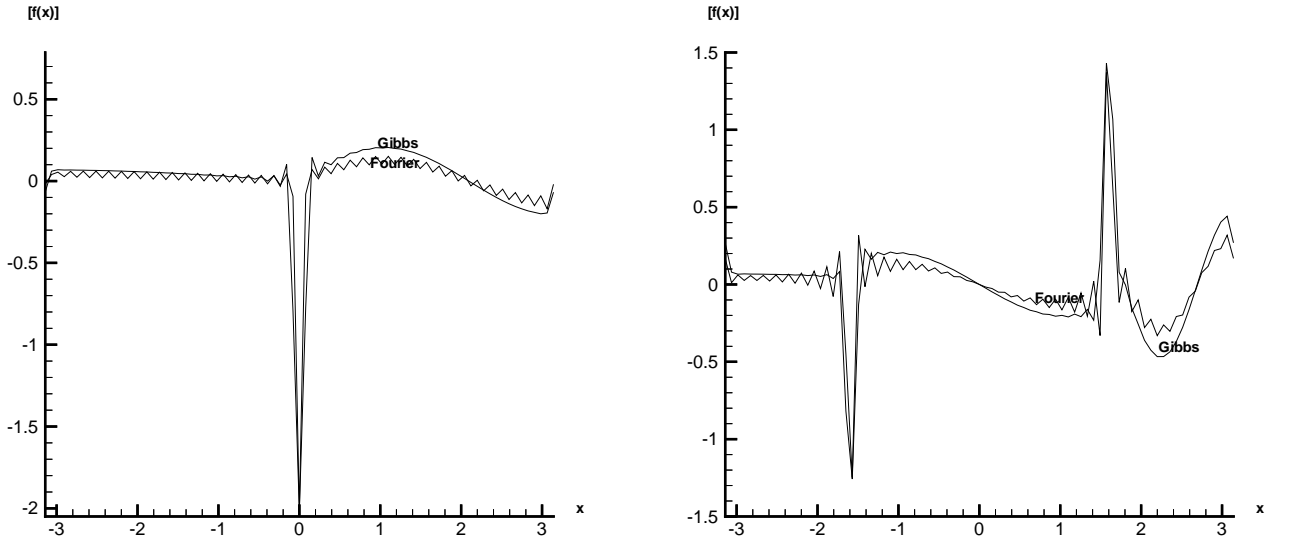


Figure 4.2: Jump value obtained by applying discrete Fourier and Gibbs concentration factors, $\tau_\alpha^F(\frac{k}{N})$ (corresponding to $\alpha = 1$ and $\alpha = \pi$) with $N = 40$ modes. The exact solutions exhibit the jump discontinuities $[f_a](0) = -2$ (on left) $[f_b](\pm \frac{\pi}{2}) = \pm \sqrt{2}$ (on the right).

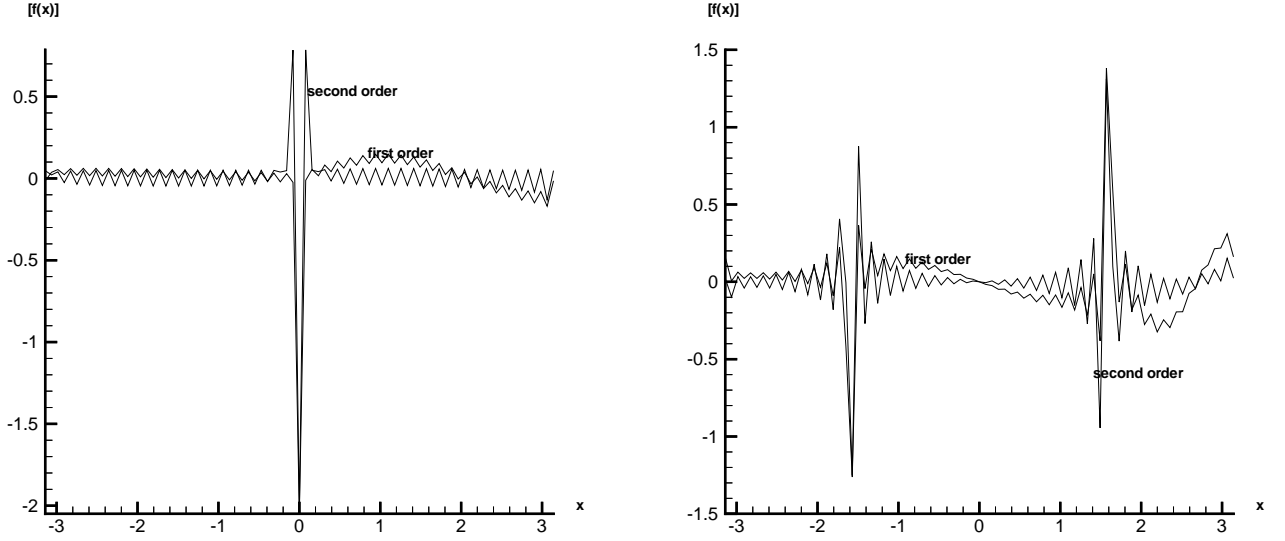


Figure 4.3: Jump value obtained by applying discrete first and second degree polynomial concentration factors with $N = 40$ modes. The exact solutions exhibit the jump discontinuities $[f_a](0) = -2$ (on left) $[f_b](\pm\frac{\pi}{2}) = \pm\sqrt{2}$ (on the right).

| N | τ_k^D | τ_k^F | τ_k^G | $\tau_k^{p_1}$ | $\tau_k^{p_2}$ |
|-----|------------|------------|------------|----------------|----------------|
| 19 | .86 | 4.3E-02 | 2.3E-02 | 9.8E-02 | 8.8E-02 |
| 39 | .90 | 2.3E-02 | 1.9E-02 | 5.0E-02 | 3.7E-02 |
| 79 | .92 | 1.2E-02 | 1.1E-02 | 2.5E-02 | 1.6E-02 |

Table 4.1: Absolute error for Example 2.1 at $x = 0$.

| N | τ_k^D | τ_k^F | τ_k^G | $\tau_k^{p_1}$ | $\tau_k^{p_2}$ |
|-----|------------|------------|------------|----------------|----------------|
| 19 | 0.20 | 0.19 | .21 | .11 | .13 |
| 39 | 0.16 | 5.9E-02 | .11 | 5.5E-02 | 6.7E-02 |
| 79 | 0.14 | 2.9E-02 | 5.4E-02 | 2.7E-02 | 3.5E-02 |

Table 4.2: Average error for Example 2.1 away from the discontinuity, $x \neq 0$.

We close this section noting that in the case of $f = f_a(x)$ in Example 2.1, Tables 4.1 and 4.2 indicate a comparable order of resolution for the different concentration factors, $\tau_k^F, \tau_k^G, \tau_k^{p_1}$ and $\tau_k^{p_2}$, both at the value at the point of discontinuity as well as the average convergence away from the point of discontinuity. For $f = f_b(x)$ in Example 3.1, however, $\tau_k^{p_1}$ produces best average errors outside the discontinuities (at $x \neq \pm\sqrt{2}$), and Figure 4.4 shows faster convergence for $\tau = \{\tau_k^{p_2}\}$, $\hat{T}_N^\tau[f](x) \rightarrow 0$ away the immediate proximity of these points of discontinuity.

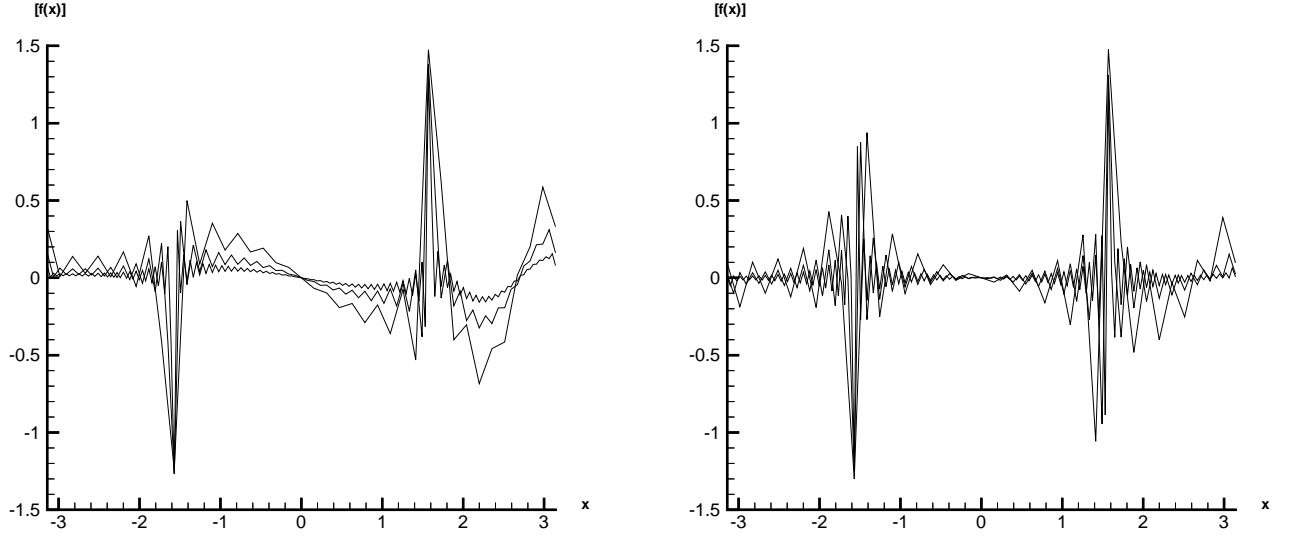


Figure 4.4: Jump value for Example 3.1 obtained by applying the first order polynomial factors, (4.16) (on the left) and second order polynomial concentration factors, (4.17), (on the right), using $N = 20, 40, 80$ modes. The exact solution 'jumps' at $[f](\pm \frac{\pi}{2}) = \pm \sqrt{2}$.

5 Concluding remarks

The theorems provided in §3 and §4 enable us to determine concentration factors for both continuous and discrete Fourier expansion coefficients that improve the overall accuracy of the concentration property of the conjugate Fourier partial sum.

It is important to mention that the choice of an appropriate concentration factor depends on various factors. Consider the following cases:

- For the one-sided mollifier proposed in [11], only the approximate jump location is required to reconstruct a piecewise continuous function, making $\sigma_k^{p_2}$ and $\tau_k^{p_2}$ appealing choices due to their rapid convergence away from the discontinuities.
- Reconstruction methods in [2] and [7] require exact knowledge of the jump locations, but in [7], for example, knowledge of the jump locations and the Fourier coefficients are enough to determine the jump discontinuities, implying that locating the jump discontinuities is more important than determining their corresponding amplitudes. This makes $\sigma_k^{p_2}$ and $\tau_k^{p_2}$ poor choices because of the strong oscillations they cause near the discontinuities.
- For highly varying functions, we have seen that $\sigma_k^{p_2}$ and $\tau_k^{p_2}$ display better results due to their rapid convergence away from the discontinuities.
- In case of several discontinuities, then $\sigma_k^{p_2}$ and $\tau_k^{p_2}$ produce too many oscillations between the points of discontinuities unless there are sufficiently many modes to 'resolve' the smooth pieces of f .
- Finally we note that the results for the Fourier concentration factors, $\sigma_\alpha^F, \tau_\alpha^F$ (with $\alpha = 1$) and the first degree concentration function, $\sigma_k^{p_1}, \tau_k^{p_1}$, bear close similarity which is not shared by the Gibbs' concentration factors, σ_k^G, τ_k^G (corresponding to $\sigma_\alpha, \tau_\alpha$ with $\alpha = \pi$). Indeed, the sensitivity of the Fourier concentration factors on the free parameter α is clearly depicted in Figure 5.1 and deserves a further study in the future.

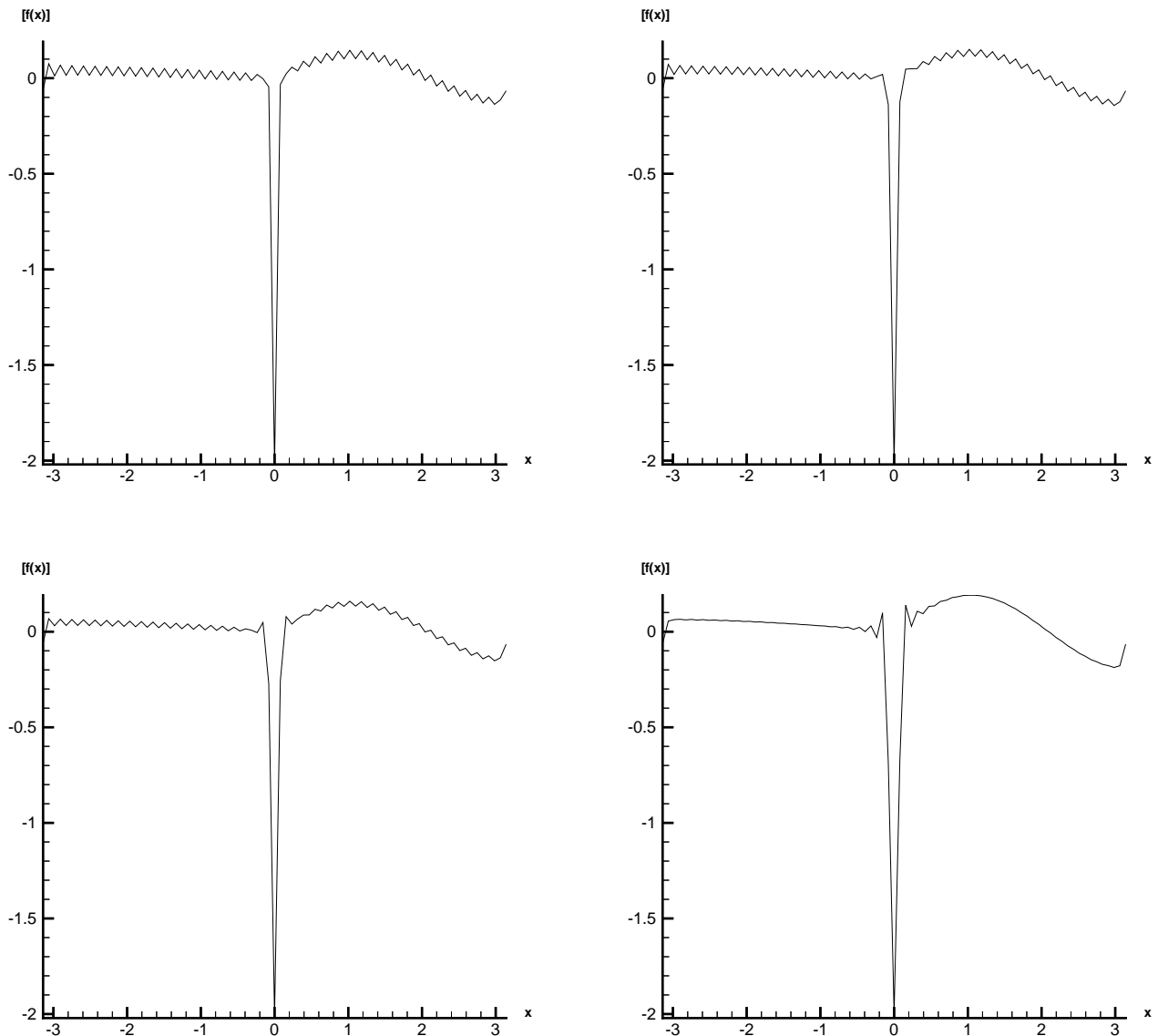


Figure 5.1: Jump value obtained by generalized conjugate partial sum, $S_{40}^\sigma[f_a](x)$ using various Fourier concentration functions $\sigma_\alpha^F(x) = \frac{-\pi}{Si(\alpha)} \sin \alpha x$, with $\alpha = 1, 1.5$ (top) and $\alpha = 2, 3$ (bottom). The exact solutions exhibit the jump discontinuity $[f_a](0) = -2$.

References

- [1] L. ALVAREZ AND J.-M. MOREL *Formulation and computational aspects of image analysis*, Acta Numerica (1994), 1–59.
- [2] N.S. Banerjee and J. Geer, Exponentially accurate approximations to piecewise smooth periodic functions, ICASE Report No. 95-17, NASA Langley Research Center, 1995.
- [3] N. Bary, *Treatise of Trigonometric Series*, The Macmillan Company, New York, 1964.

- [4] H.S. Carslaw, *Introduction to the Theory of Fourier's Series and Integrals*, Dover, 1950.
- [5] I. Daubechies, *Ten Lectures on Wavelets*, CBMS-NSF, 1992.
- [6] R. DeVore and B. Lucier, *Wavelets*, *Acta Numerica* 92, (1992), pp. 1–56.
- [7] K.S. Eckhoff, Accurate reconstructions of functions of finite regularity from truncated series expansions, *Math. Comp.* **64** 671-690 (1995).
- [8] K.S. Eckhoff and C. E. Wasberg, *On the numerical approximation of derivatives by a modified Fourier collocation method*, Rep. No. 99, Department of Mathematics, University of Bergen, Norway, 1995.
- [9] D. Gottlieb and E. Tadmor, *Recovering Pointwise Values of Discontinuous Data within Spectral Accuracy*, in "Progress and Supercomputing in Computational Fluid Dynamics", Proceedings of a 1984 U.S.-Israel Workshop, Progress in Scientific Computing, Vol. 6 (E. M. Murman and S. S. Abarbanel, eds.), Birkhauser, Boston, 1985, pp. 357-375.
- [10] D. Gottlieb and C.-W. Shu, On the Gibbs phenomenon and its resolution, *SIAM Review*, 1997.
- [11] D. Gottlieb, C.-W. Shu, A. Solomonoff and H. Vandeven, *On the Gibbs phenomenon I: recovering exponential accuracy from the Fourier partial sum of a nonperiodic analytic function*, *J. Comput. Appl. Math.* 43, (1992) pp. 81-92.
- [12] Y. Maday, S. M. Ould Kaber and E. Tadmor *Legendre pseudospectral viscosity method for nonlinear conservation laws*, *SIAM Journal on Numerical Analysis* 30 (1993), 321-342.
- [13] A. Majda, J. McDonough and S. Osher, The Fourier method for nonsmooth initial data, *Math. Comp.* 30 (1978), pp. 1041-1081.
- [14] S. Mallat, Multiresolution approximations and wavelets orthonormal bases of $L^2(R)$, *Trans. Amer. Math. Soc.* 315 (1989), pp. 69-87.
- [15] Y. Meyers, *Wavelets, algorithms and applications*, SIAM, 1993.
- [16] E. Tadmor, Convergence of spectral methods for nonlinear conservation laws, *SIAM J. on Numer. Anal.* 26 (1989), pp. 30-44.
- [17] H. Vandeven, *Family of spectral filters for discontinuous problems*, *SIAM J. Sci. Comput.* 48 (1991), pp. 159-192.
- [18] A. Zygmund, *Trigonometric Series*, Cambridge University Press, 1959.